THE ASTROPHYSICAL JOURNAL, 397:362–380, 1992 October 1

EFFECT OF BINARY SOURCES ON THE SEARCH FOR MASSIVE ASTROPHYSICAL COMPACT HALO OBJECTS VIA MICROLENSING

KIM GRIEST
Center for Particle Astrophysics and Astronomy Department, University of California, Berkeley, CA 94720
AND
WAYNE HU
Physics Department, University of California, Berkeley, CA 94720
Received 1992 March 4; accepted 1992 April 7

ABSTRACT

If the dark matter in the Galactic halo consists of compact objects in the 10^{-6}–10^{2} $M_{\odot}$ mass range, it can be detected as it gravitationally microlenses stars in neighboring galaxies and the Galactic bulge. Though extremely rare, microlensing has several powerful signatures: the light curves follow a well-known function, are time symmetric, and are the same in all filter bands. These signatures, however, may be lost if the source star is a member of a binary system. Since most stars are, in fact, members of binaries, the true microlensing events may be rejected as background. We study the effect of binary sources by using the event geometry and resulting light curves to define several categories of binary microlensing events, and then calculate the probability of each category occurring. We average these probabilities over measured distributions of binary orbital periods and mass ratios, finding $\sim$10%–20% of events on binary sources should be distinguishable from single-source microlensing events (for the LMC). The bulk of binary events should be achromatic and similar to single source light curves, but 2%–5% should have truly unusual light curves and color shifts greater than 0.1 mag. The total microlensing rate is larger by 5%–15% for binary sources and in deriving the MACHO mass from a binary light curve an error of a factor of 2 or more may be made if single source formulae are used.

Subject heading: gravitational lensing

1. INTRODUCTION

In 1986, Paczyński (1986) suggested searching for the dark matter thought to exist in the halo of the Galaxy by watching for microlensing of stars in the Large Magellanic Cloud (LMC). He found that MACHOs (massive astrophysical compact halo objects) in the mass range $\sim 10^{-8}$–10^{2} $M_{\odot}$ (planets, jupiters, brown dwarfs, black holes, etc.) could be discovered or ruled out if $\sim 10^{6}$ stars in the LMC were monitored for several years. As a MACHO comes close to the observer-source (star) line of sight, it acts as a gravitational lens, producing two images. While the angular separation between the two images is typically too small to allow them to be resolved, an apparent increase in the brightness of the source results and can be large (Paczyński 1986; Griest 1991). The duration, t_e, of the brightening depends upon the mass of the MACHO and on its velocity transverse to the line of sight, but typically ranges from a few hours for 10^{-6} $M_{\odot}$ MACHOs, to several years for 100 $M_{\odot}$ MACHOs.

Since Paczyński's work, several groups (Alcock et al. 1991; Ferlet et al. 1990; Paczyński et al. 1991) have embarked on serious attempts to find (or rule out) baryonic dark matter using this technique. While this technique is very promising, it has several potential problems. Since the microlensing of a given star is so rare, a huge number of photometric measurements must be made and the analysis must be completely automated. Thus the potential of systematic error or background causing apparent brightening of stars is worrisome. It has been pointed out (Paczyński 1986; Alcock 1989; Griest 1991) that while the potential background may be large compared to the estimated signal, microlensing events have several unique features which serve as signatures.

1. Since microlensing is so rare, an event should happen only once on a given star. If a star continues to vary it can be identified as a variable star and left out of the source sample.
2. The light curve of a microlensing event is symmetric in time. (The rise is the same as the fall.)
3. The light curve of a microlensing event is achromatic. Since the Alcock group plans to image stars in two colors simultaneously, flare stars and other transient brightenings which also give a change in the color of the object can be eliminated by demanding chromaticity.
4. While the duration and peak amplification[1] of a microlensing event depend upon the unknown MACHO mass, impact distance, and transverse velocity, the shape of the light curve is a well-known function of these parameters. Thus a brightening which cannot be fit with this specific function can be rejected. This also allows one to estimate the mass of the MACHO from the duration of the event.[2]
5. Since the maximum amplification is a function *only* of the scaled distance of closest approach of the MACHO to the line of sight, if many events are found, they should follow a known distribution of maximum amplification: $dN/dA_{\max} \sim 1/A_{\max}^2$ ($A_{\text{threshold}} < A_{\max} < \infty$; see Griest 1991 for a more accurate formula). This distribution is independent of MACHO mass and velocity, source star brightness and color, etc. In fact the

[1] We will use the word "amplification" throughout, even though "magnification" might be more correct.
[2] The duration actually depends on a combination of the MACHO mass, distance, and velocity. Since the MACHO velocity and distance are not known, deduction of MACHO masses can only be made statistically once a velocity and density distribution have been assumed.

microlensing rate in general is independent of the source star brightness and color.

Given the large number of unique signatures, it is hoped that the microlensing "needles" can be picked out of the background "haystack," and if nothing is found, that a strong statement concerning the viability of MACHO dark matter can be made.

However, it has been pointed out (Paczyński 1986; Alcock 1989; Spiro 1990; Griest 1991) that the above signatures are valid only for pointlike sources and that they may not hold for giant star sources, or for sources which are members of binary systems. Giant stars are not pointlike, and the amplification light curve formulae mentioned above, break down when the projected Einstein ring radius becomes smaller than the source radius. This effect has been studied by Paczyński (1986), Milsztajn (1990, unpublished), Bennett (1990, unpublished), Griest & Hu (1990, unpublished), and Jetzer (1991), and for MACHOs above $\sim 10^{-6}\ M_{\odot}$ (at the LMC distance) is not an important effect. For lower mass MACHOs, or sources in the Galactic bulge, this can be a serious effect. However, we will not discuss giant stars here.

Binary sources present a potentially more serious problem.[3] As pointed out by Spiro (1990) and Griest (1991), and detailed in this paper, a binary source can destroy most, if not all, of the signatures discussed above. A microlensing event taking place on a binary source may not be symmetric in time, or follow anything close to the normal light curve shape. It can have two peaks or be very asymmetric. If the two stars of the binary system have different colors, and only one is lensed, the apparent color of the unresolved system will change as a function of amplification, and the achromaticity signature may be lost. Thus genuine microlensing events may be rejected. Also, when binary sources are lensed and fit to a single source light curve, the relationship between event duration and MACHO mass and velocity can be changed considerably. This is the case even when the shape of the light curve is indistinguishable from a single source microlensing light curve. If both stars are lensed the event may have a longer duration than a single star light curve with the same amplification, while if only one star is lensed the duration will be shorter than expected. Finally, the distribution of events as a function of maximum amplification can change. Since the fraction of stars which are members of binary (or multiple) star systems is estimated to be very large (60%–100%) (Abt 1983), it seems that a study of the effect of binary sources on microlensing detection is warranted. In this paper we study this effect.

In § 2 we set up some formalism necessary to discuss microlensing of binary sources. In § 3 we use this formalism to categorize and discuss the different types of binary light curves. We define several categories of light curves: "offset bright" events, where only the bright star is lensed, "offset dim" events, where only the dim star is lensed, "effectively single" events, where both stars are lensed, but they are so close together that the light curve is indistinguishable from a single source light curve, as well as "double-peaked events", "asymmetric events," "merged offset dim events" and "borderline events." We display example light curves for each category, and using simple geometry show how each category arises. In § 4 (and in the Appendix) we calculate the total rate of microlensing of binary sources (it is larger than the single source rate), and we find the probability of each category of event occurring as a function of d, the projected scaled distance between the two stars, and $r = L_2/(L_1 + L_2)$, the luminosity offset ratio. (L_1 is the apparent luminosity of the bright star and L_2 is the apparent luminosity of the dim star. In § 5 we attempt to make contact with observation by averaging the probabilities found in § 4 over realistic distributions of d and r. While a great deal of data exist on the duplicity of stars and their distribution in orbital period and mass ratio, we find no clear consensus on the total binary frequency or on the actual distributions we require. So we leave the total duplicity as a free parameter and use three different observational determinations of these distributions. We take the differences arising as a result of using the three different distributions as a measure of the uncertainty of our conclusions. We find, perhaps somewhat surprisingly, that while binarity gives a measurable effect, it does not give an overwhelming effect for binaries in the LMC, and that the unusual light curves, discussed in § 3 should be in fact relatively rare. For the best determined distributions (Duquennoy & Mayor 1991), in systems that are binary, light curves which are easily distinguishable from single source light curves should occur only 2%–5% of the time, while events which might be distinguished with good data should occur perhaps 10%–20% of the time. Events which are "effectively single" both in color and light curve shape occur roughly 3%–30% of the time depending on the MACHO mass, while the most common type of event is the "offset bright," occurring 50%–75% of the time. We also find that the total rate of microlensing is increased by binaries (compared to the rate if all stars were singles), but only by $\sim$5%–15% (depending on MACHO mass and which binary data we use).

In § 6 we briefly consider the probability of achromatic microlensing events. We find some interesting color shifting light curves, but conclude that these too are also fairly rare, less than roughly 5% of events involving binary sources should have a shift in $B-V$ magnitude of more than 0.1 mag. This is mostly because it is rare to find stars of nearly equal magnitude with different colors. In § 7 we discuss the miscalculation made in deriving the MACHO mass using the single source formulas for binary light curves. For offset dim events the error can be an order of magnitude or more, but these events should be recognizable as being due to binary microlensing. For offset bright events, which are probably indistinguishable from single source light curves, the error is of order 5%–10%, and averaging over all types of events one would expect to make up to a factor of 2 error in MACHO mass if one ignored binarity. Finally, in § 8, we briefly discuss the effect of binary motion, finding new types of light curves such as those having periodic "ripples" on them. We estimate, however, that this type of event should be quite rare.

2. MICROLENSING OF BINARY SOURCES

In this section we recall some of the formulae of point source microlensing and develop some nomenclature.

We define microlensing as occurring if the total brightness of a source increases by more than a factor A_T. (Equivalently, if the magnitude of the source decreases by more than $\Delta m_T = -2.5 \log A_T$.) The duration of an event t_e is defined as the time for which $A \geq A_T$. The amplification (more properly

[3] Throughout we will be considering binary systems whose members are gravitationally bound. However, many of the results of this paper are unchanged if one considers "optical binarieis," that is, stars which are by chance near each other on the sky, but not members of the same system. Of course the measured distributions we use are for bound systems.

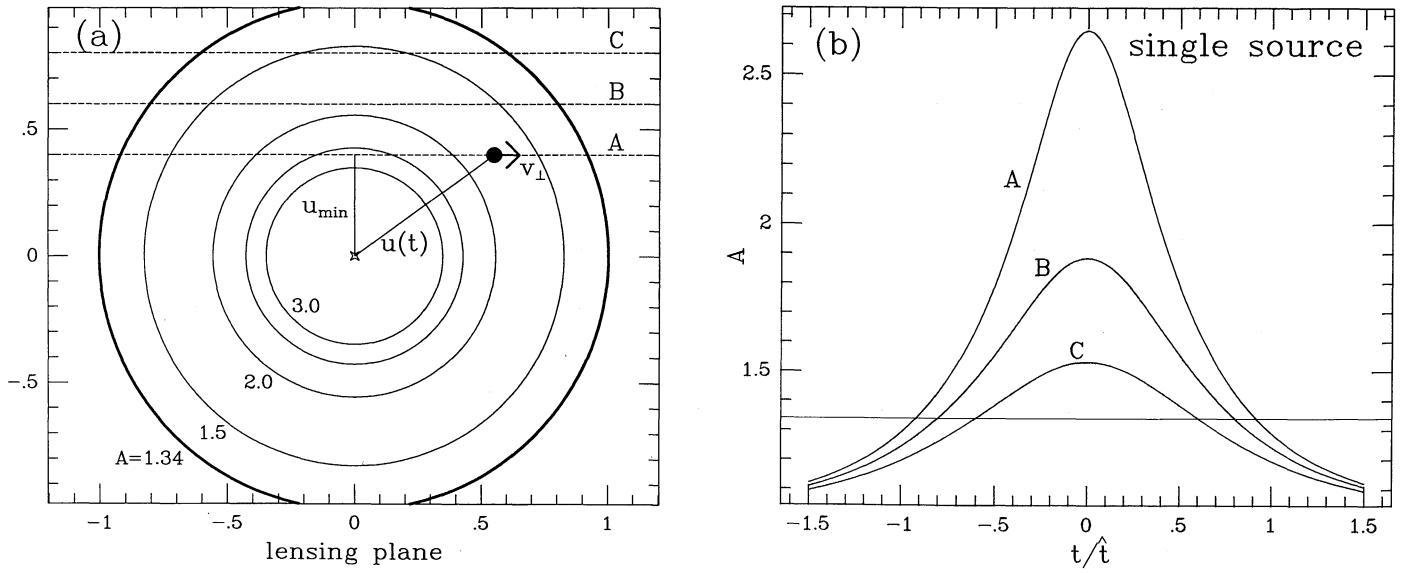

FIG. 1.—Point source (nonbinary) microlensing geometry and light curves. The light curves corresponding to the three trajectories shown as labeled dashed lines in part (*a*) are displayed in part (*b*). In part (*a*) contours of amplification $A = 1.34$ (*dark solid line*), 1.5, 2, 2.5, and 3 are shown. In part (*a*) the MACHO and its transverse velocity are shown, as are the parameters u_{min} and $u(t)$. The ordinate and abscissa are in units of the Einstein radius. In part (*b*) a line is drawn at $A_T = 1.34$ to indicate the onset of an event.

magnification) is given by

$$A(u) = \frac{u^2 + 2}{u(u^2 + 4)^{1/2}} \approx \frac{1}{u}, \tag{1}$$

where the approximation is valid for $A \gtrsim 2$ or $u \lesssim 0.5$. The dimensionless distance to the line of sight is

$$u(t) = b/R_e = [u_{min}^2 + (t/\hat{t})^2]^{1/2}, \tag{2}$$

where b is the distance to the line-of-sight and R_e is the Einstein ring radius (see Fig. 1). The maximum amplification A_{max} is defined to occur at time $t = 0$, and is set by $u_{min} = b_{min}/R_e$. The characteristic time is $\hat{t} = R_e/v_\perp$, where $v_\perp$ is the MACHO speed tranverse to the line of sight. The basic lensing scale is set by the Einstein ring radius

$$R_e = 0.61\left[\frac{m}{10^{-6}\,M_\odot}\frac{L}{\text{kpc}}x'(1-x')\right]^{1/2} R_\odot,$$
$$= 8.0\left[\frac{m}{M_\odot}\frac{L}{50\text{ kpc}}\frac{x'}{0.2}\left(\frac{1-x'}{0.8}\right)\right]^{1/2}\text{a.u.}, \tag{3}$$

where m is the MACHO mass, L is the distance to the source ($L = 50$ kpc for the LMC), and $x' = x/L$, where x is the distance to the MACHO from the observer. For the typical microlensing of a star in the LMC by dark matter in the Galactic halo, $x' \approx 0.2$, (Paczyński 1986), but see Griest (1991) for a more accurate treatment. We also define the scaled threshold distance u_T as the u corresponding to A_T,

$$u = 2^{1/2}[A(A^2 - 1)^{-1/2} - 1]^{1/2}.$$

A convenient threshold amplification is $A_T = 1.34$ which corresponds to $u_T = 1$, i.e., an event is defined as taking place whenever the star (projected on the lensing plane) is within the Einstein ring. Note that $A = A_T$ takes place at $t = \pm t_e/2$, so $u_T^2 = u_{min}^2 + (t_e/\hat{t})^2/4$, and that a point source microlensing light curve is completely determined by specifying the time of its peak amplification and any three of the four parameters: A_T, A_{max}, t_e, and $\hat{t}$. Thus if we set a threshold, and measure A_{max} and t_e, we can determine $\hat{t}$. Also note that the light curve is symmetrical in time ($t \to -t$) and if the source were observed in several filter bands, the amplification would be identical in all bands. Finally, since A_{max} is determined only by u_{min}, and u_{min} is distributed at random between 0 and u_T, for events with $A > A_T$, the fraction of events which occur with u_{min} between u and $u + du$ is just $dN = du/u_T$, and so the fraction of events with amplification between A and $A + dA$ is $dN = u_T^{-1}(du/dA)dA$ (see Fig. 10 of Griest 1991). Figure 1 illustrates the geometry for three sample trajectories (labeled A, B, and C) and shows the resulting light curves (for a point source). Distances in the lensing plane are all divided by R_e. The threshold line drawn at $A = 1.34$ in Figure 1*b* indicates the onset of the events.

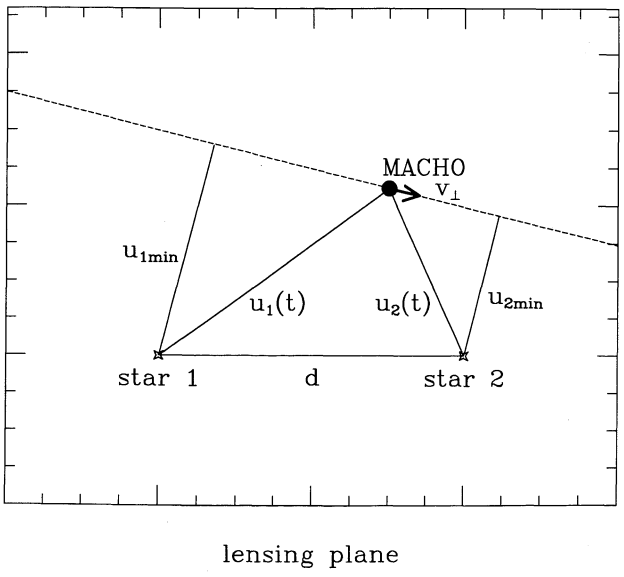

FIG. 2.—Geometry of binary microlensing. All distances are in the lensing plane and are divided by the Einstein radius R_e.

When the source consists of two stars, a similar analysis can be done. Consider two pointlike sources separated by a distance D and of apparent luminosities L_1 and L_2 (in V band for example). If the stars are at a distance L from the observer and the MACHO is at a distance x, then the Einstein radius is given approximately by the last line of equation (3), $R_e \approx 8(m/M_\odot)^{1/2}$ a.u. (for MACHOs in a Maxwellian dark matter halo and stars in the LMC). Note $[x'(1-x')]^{1/2}$ varies little as x' varies from 0.2 to 0.8, and we will use $x' = 0.2$ as typical throughout this paper. In the plane of the lens let the scaled projected distance between the stars be $d = Dx'/R_e \approx D/(40\sqrt{m/M_\odot})$. As the MACHO moves close to the observer-star lines of sight, each point source is independently amplified by $A_1 = A_1(u_1)$ and $A_2 = A_2(u_2)$ respectively, where $A(u)$ is given in equation (1), and u_1, u_2 are the projected, scaled distances to the lines of sight. This geometry is shown in Figure 2. When the MACHO is far away, the total apparent luminosity of the system is $L_1 + L_2$, so the total amplification is

$$A_{\rm tot} = \frac{A_1 L_1 + A_2 L_2}{L_1 + L_2} = A_1(1-r) + A_2 r\,, \tag{4}$$

where we have defined the luminosity offset ratio,[4]

$$r = L_2/(L_1 + L_2)\,. \tag{5}$$

Without loss of generality, we take $L_2 \le L_1$, so $0 \le r \le 0.5$ (star 2 is the dimmer star). Thus for any given MACHO trajectory we can easily find the total increase in brightness as a function of time.

When the two stars have different colors, there are then two luminosity offset ratios, one for each color. For example, consider star 1, with an apparent luminosity L_{1V} in the V-band, and L_{1B} in the B-band. ($V = -2.5 \log L_{1V} + \text{constant}$, and likewise for B.) We can then define

$$r_V = \frac{L_{2V}}{L_{1V} + L_{2V}} = (1 + 10^{(V_2 - V_1)/2.5})^{-1}\,,$$
$$r_B = \frac{L_{2B}}{L_{1B} + L_{2B}} = (1 + 10^{(B_2 - B_1)/2.5})^{-1}\,. \tag{6}$$

Now suppose star 1 has color $B_1 - V_1$, and star two has color $B_2 - V_2$. Then the system will have total color

$$(B-V)_{\rm tot} = -2.5 \log [(L_{1V} + L_{2V})/(L_{1B} + L_{2B})]\,.$$

As microlensing proceeds,

$$L_{1V} \to L_{1V} A_1\,, \quad L_{1B} \to L_{1B} A_1\,,$$
$$L_{2V} \to L_{2V} A_2\,, \quad L_{2B} \to L_{2B} A_2\,, \tag{7}$$

so the total color change is $\Delta(B-V) = 2.5 \log A_{B-V}$, where

$$A_{B-V} = \frac{(1-r_V)A_1 + r_V A_2}{(1-r_B)A_1 + r_B A_2}\,. \tag{8}$$

Once again, a given MACHO trajectory defines $u_1(t)$ and $u_2(t)$, from which $A_1(t)$ and $A_2(t)$ can be found and from these one finds the change in color as a function of time. Note that if the two stars have the same color, then $r_V = r_B$ and $\Delta(B-V) = 0$ as expected. Also, whenever both stars are amplified by the same amount ($A_1 = A_2$), $\Delta(B-V) = 0$.

[4] A MACHO which lenses only one star produces a light curve much like a single source light curve, except that the amplification is "offset" from its single source value due to the other star. The amount of the offset is determined by the "luminosity offset ratio" r. We will denote such microlensing events as "offset" events.

3. CATEGORIES OF BINARY EVENTS

A way of displaying all of the possible binary microlensing light curves is to draw a contour plot of amplification A in the lensing plane. This shows the value of $A_{\rm tot}$ which would be obtained if a MACHO lay at each point in the plane (at a distance u_1 and u_2 from the sources). A light curve is then just a slice or trajectory through this contour plot. Figure 3 shows contours (*solid lines*) of $A = 1.34$, 1.5, 2.0, 2.5, and 3.0 for stars separated by $2R_e$ ($d = 2$), in the lensing plane (see Fig. 2) with $r = 0.1$ (dim star 9 times fainter than the bright star). Figure 4 shows the same contours for the same value of r, but for stars separated by $1.6R_e$ ($d = 1.6$). Figures 5 and 6 show the same for $d = 0.7$ and $d = 0.25$, respectively. Most of the interesting effects can be deduced from these figures.

Consider first Figure 3, where the stars are separated by more than an Einstein radius (in the lensing plane). The dark $A = 1.34$ threshold contours are distinct circles around each star. Thus for this case there are only three possible types of microlensing events. "Offset bright": the MACHO trajectory passes through only the bright star threshold contour; "offset dim": the MACHO trajectory passes through only the dim star threshold contour; and "separated double-peak" events: effectively two distinct microlensing events, where the trajectory passes first through one and then the other threshold circle.

The straight lines in Figure 3*a* show several possible trajectories (labeled A, B, C, D, E, and F), and the resulting light curves are shown in Figures 3*b*, 3*c*, and 3*d*. The solid lines in Figures 3*b* and 3*c* show the binary light curves, while the dashed lines show the unique single source light curve which has the same duration and maximum amplification. A line is drawn at $A = 1.34$ to indicate the onset of an event. The differences between the solid and dashed lines indicate the "distinguishability" of the binary light curves. For the offset bright light curves shown in Figure 3*b*, above threshold, the solid and dashed lines fall almost on top of each other, so an observer who measured such a light curve would have difficulty distinguishing it from a single source light curve. However, even when the binary light curve is indistinguishable from a single source light curve, the relationship between the duration and the MACHO mass has been changed, and the observer would make a mistake in deducing the MACHO mass using the single source formulae (as will be discussed in § 7.)

Figure 3*c* shows two offset dim light curves (trajectories C, D). Curve (C) illustrates that for high amplification events, offset dim light curves are quite different from single source light curves, and easily distinguishable. (Of course an inappropriately programmed computer might have trouble and might reject such an event as not being caused by microlensing). A low amplification dim offset event, however (trajectory D), may be more difficult to distinguish. Also, clearly as r approaches 0.5, offset dim and offset bright events become the same, rendering the distinction meaningless. (When $r = 0.5$, both offset dim and offset bright events look fairly similar to single source events.)

Figure 3*d* shows separated double-peaked events (trajectories F and G), clearly identifiable as double star microlensing events.

Next consider Figure 4. Here, while the stars are still farther

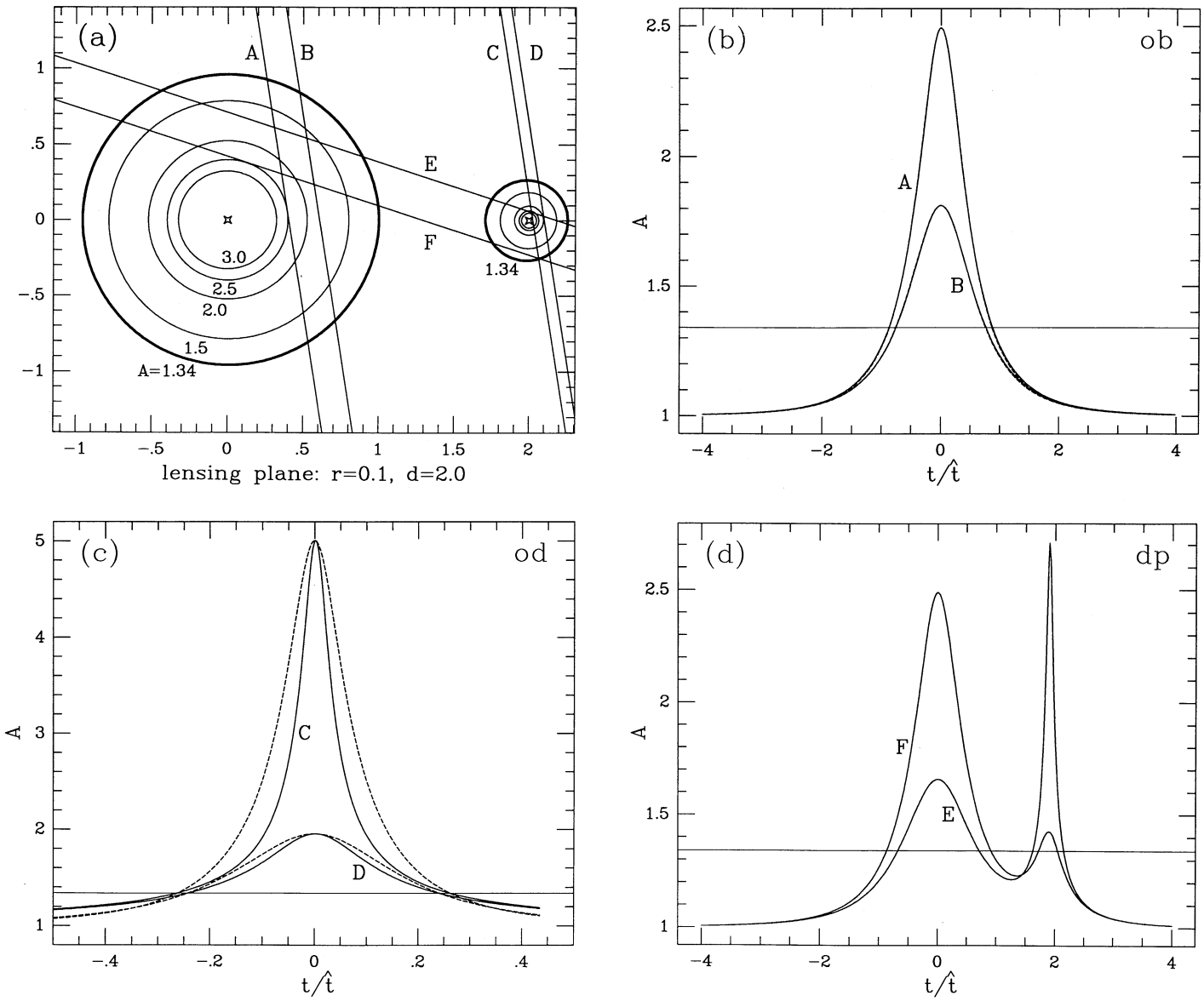

FIG. 3.—Amplification contour plots, MACHO trajectories, and the resulting light curves for binary sources. Part (*a*) shows contours of total amplification A in the lensing plane for $d = 2.0$ and $r = 0.1$; $A = 1.34$ (*dark solid lines*), 1.5, 2, 2.5, and 3. Several MACHO trajectories are labeled (A), (B), etc. (*straight solid lines*). Parts (*b*), (*c*), and (*d*) show the light curves resulting from the labeled trajectories. Part (*b*) shows trajectories (A) and (B) (offset bright events), part (*c*) shows trajectories (C) and (D) (offset dim events), and part (*d*) shows trajectories (E) and (F) (double-peaked events). In parts (*b*) through (*d*) the solid lines are binary light curves, while the dashed lines (where shown) are the single source light curves with the same peak amplification and duration. The threshold value $A_T = 1.34$ is indicated by the horizontal lines in parts (*b*)–(*d*).

than u_T apart (for $A_T = 1.34$, the threshold radius u_T corresponds to an Einstein radius), the concentric threshold circles have merged, with a bridge forming between them. Three trajectories and the corresponding light curves are shown. Categorization in this transitional case is ambiguous and we return to this case after considering Figures 5 and 6.

In Figure 5 ($d = 0.7$ and $r = 0.1$), the projected separation of the stars is comparable to the Einstein ring radius, so typically both stars are involved in microlensing events. The contours (*solid curved lines*) show more complicated structure, and so more complicated light curves can result. In trying to categorize possible types of events, we need a measure of how near a MACHO must come to a binary system so that its binary nature is probed. When the MACHO passes far from a binary source its microlensing light curve is indistinguishable from a single star light curve. Correspondingly, low-amplification contours are circles centered around the binary system. On the other hand when a MACHO passes sufficiently close to one member of a binary, the microlensing event may be described by considering the companion as merely background. Therefore very high amplification contours are two independent circles centered around the respective stars. Going from low amplifications to high amplifications the single connected contour "pinches off" to become two disconnected contours. The value of amplification $A_{\rm pinch}$ at which this pinching-off occurs and its corresponding (via eq. [1]) pinch-off distance $u_{\rm pinch}$, thus provides an intuitive and convenient measure of the extent to which binarity is probed. At distances closer than the

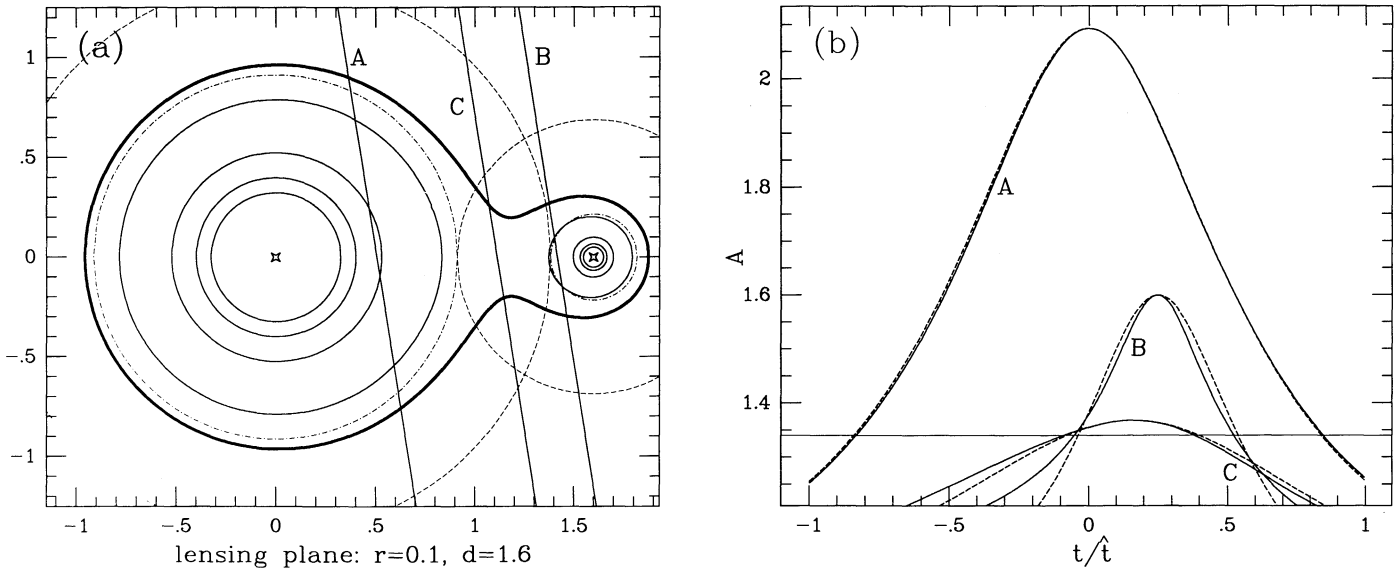

FIG. 4.—Same as Fig. 3 for $d = 1.6$. Pinch-off circles are shown as dot-dashed curves, while the larger influence circles are shown as dashed curves. Trajectory (A) is an ob event, (B) is an mod event, and (C) is missed (see text).

pinch-off distance a star's influence completely dominates the light curve. The pinch-off amplification can be found numerically and $u_{\rm pinch}$ found from equation (1), but we find that the empirical relation

$$\left(\frac{d-u_{\rm pinch}}{u_{\rm pinch}}\right)^s+\left[\frac{(1/2)-r}{1/2}\right]^s=1\,, \tag{9}$$

fits quite well, and we will use it throughout the paper. We found numerically that $s \approx 2$ for $A > 2$ and rises to $s \approx 2.2$ for $A = 1.34$. This expression may easily be solved to obtain:

$$u_{\rm pinch}=\frac{d}{[1-(1-2r)^s]^{1/s}+1}\,. \tag{10}$$

We thus can divide binary microlensing events into two broad categories: separated threshold events, when $u_{\rm pinch} > u_T$, and merged threshold events when $u_{\rm pinch} < u_T$. For the separated threshold events already illustrated in Figure 3*a*, the threshold contours can be approximated as two circles whose radii can be found by treating the companion star as background ($A_2 = 1$ for star 1, and $A_1 = 1$ for star 2)

$$\begin{aligned} A_{1T}&=\frac{1}{1-r}\,(A_T-r)=1+\frac{A_T-1}{1-r}\\ A_{2T}&=\frac{1}{r}\,(A_T+r-1)=1+\frac{A_T-1}{r}\,, \end{aligned} \tag{11}$$

where the radii are $u_{1T} = u(A_{1T})$ and $u_{2T} = u(A_{2T})$.

For the merged threshold situation shown in Figure 5*a*, we likewise define independent "pinch-off" circles from

$$A_{1\rm pin}=\frac{1}{1-r}\,(A_{\rm pinch}-r)\,,\quad A_{2\rm pin}=\frac{1}{r}\,(A_{\rm pinch}+r-1)\,, \tag{12}$$

with pinch-off radii $u_{1\rm pin} = u(A_{1\rm pin})$, and $u_{2\rm pin} = u(A_{2\rm pin})$. We find that when a MACHO is inside a star's pinch-off circle, the microlensing light curve is completely dominated by that star and the companion can be treated as background. When a MACHO passes through both pinch-off circles a double-peaked light curve results, as illustrated by trajectory (D) in Figure 5*c*. The region of influence of a star, within which it has the ability to distort significantly the light curve, extends to a larger region than the pinch-off circle, however. In the direction of the other star it extends, in fact, to the point at which its companion becomes dominant, i.e., until entering the companion's pinch-off circle. Therefore we define two "influence circles" with radii

$$u_{1\rm inf}=d-u_{2\rm pin}\,,\quad u_{2\rm inf}=d-u_{1\rm pin}\,. \tag{13}$$

When a MACHO is inside the influence circle of a star, the amplification is influenced by that star. Note that whenever the MACHO is inside the pinch-off circle of one star, it is by definition, outside the other star's influence circle. Also note that when $u_{1\rm inf} > u_{1T}$ or $u_{2\rm inf} > u_{2T}$, we do not need to use influence circles, since no event is taking place in this case. We simply use the threshold circles. In the figures pinch-off circles are drawn in dot-dashed lines and the large influence circles are drawn in dashed lines.

Using the pinch-off and influence circles we can categorize binary microlensing events in more detail. For example, trajectory (A) in Figure 5 enters the influence and pinch-off circle of star 1, but never enters either the influence or pinch-off circle of star 2. So this will produce an event with an "offset bright" light curve similar in properties to the curve shown in Figure 3*b*. This is shown if Figure 5*b*. Just as before, this light curve is hard to distinguish from a single source light curve, but the determination of the MACHO mass will be off, especially if $r \approx 0.5$. Trajectory (B) passes only within star 2's influence circle, so we call it a "merged offset dim" event. The resulting light curve is shown in Figure 5*b*, and is seen to be similar to the offset dim curve in Figure 3*c*. However, there is an extra "shoulder" seen in Figure 5*b*. This is why we separate the "offset dim" and "merged offset dim" categories. Next, trajectory (C) passes through *both* influence circles, but neither pinch-off circle, and is never completely influenced by only one star, yet it also never switches influences circles. Such events are equally influenced by both stars and result in roughly symmetric light curves such as shown in Figure 5*b*. We will lump

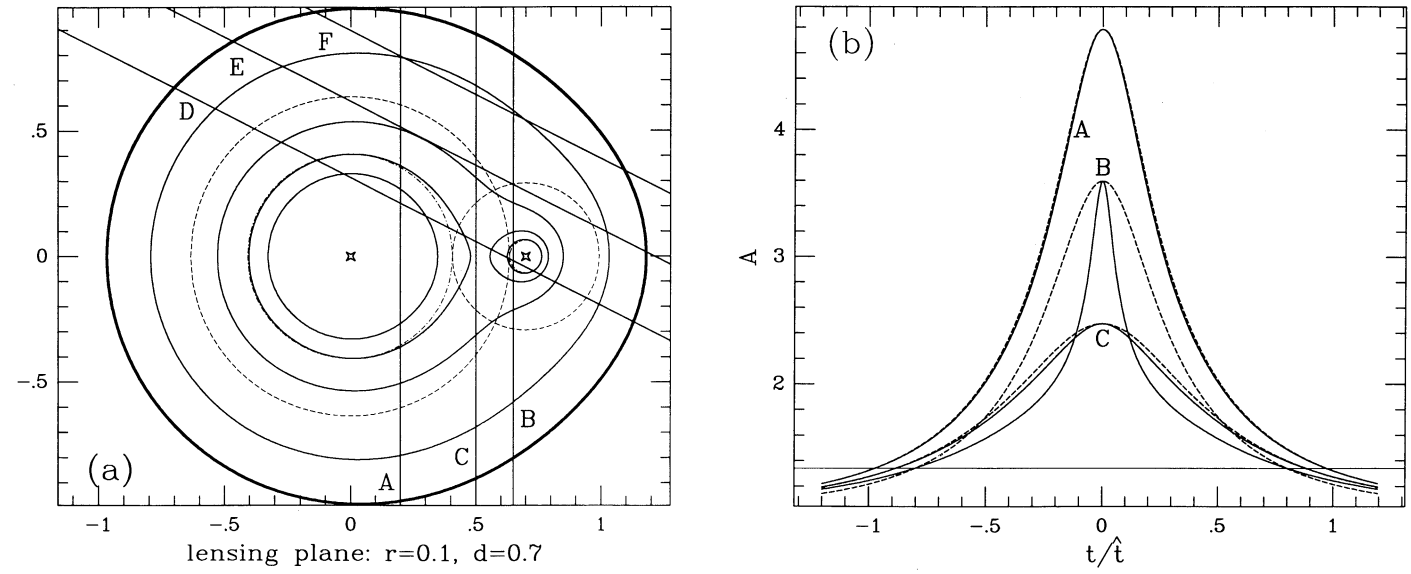

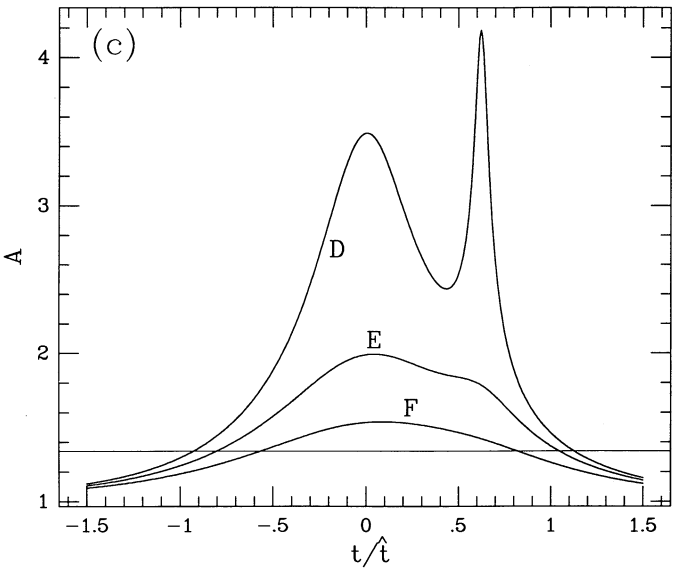

FIG. 5.—Same as Fig. 3 and 4 for $d = 0.7$. Trajectory (A) is an offset bright, (B) is a merged offset dim, (C) is a borderline, (D) is a double-peaked, (E) is an asymmetric, and (F) is a borderline event.

this type of event with events which enter *neither* influence circle and call them "borderline" events, a catch-all category for events which lie between our other, more obvious categories. As can be seen from the light curve, this event is also on the borderline of being distinguishable by shape from a single source light curve, though again, the relationship between mass and event duration is modified.

As mentioned, trajectory (D) passes through both pinch-off circles and results in a double-peaked event shown in Figure 5*c*. Trajectory (E) passes through the influence circle of star 1 and then through the influence circle of star 2. It is first under the influence of star 1 (inside influence circle 1, and *not* inside influence circle 2), and then under the influence of star 2. The resulting light curve is shown in Figure 5*c*. Events such as the one shown in trajectory (E), which switch influence circles, but do not qualify as "double-peaked" by entering *both* pinch-off circles, typically give rise to single-peaked, but recognizably asymmetric light curves, and will be denoted "asymmetric events." They are easily distinguished from single source light curves. Lastly, trajectory F passes through neither circle of influence, but yet does not get inside the $A_T = 1.34$ threshold contour. As mentioned previously, and as evidenced from its light curve, this is a "borderline" event. It has low peak amplification and would be hard to detect, but with good data it might be distinguishable from a single source event.

Next, consider Figure 6, where the projected star separation is only $0.25R_e$ (still with $r = 0.1$). Here trajectory (A) results in an asymmetric event shown in Figure 6*b*, while trajectory (B) falls outside both influence circles and so is categorized as borderline. Trajectory (C) is a new case. Here, the trajectory is so far from the individual influence circles (but still within the $A_T = 1.34$ contour) that the amplification contours are nearly circular. Such trajectories do not probe the binary nature of the source in any way, and so we call them "effectively single." Both the light curve and color shift will be given approximately by the single source formulae and no correction to the mass-duration relationship will be needed. By trial and error, we find a radius of $d = 2$ to be a reasonable boundary between "effectively single" and "borderline" events. Trajectories which do not pass within $d = 2$ of the center of the system will be called effectively single.

Finally, reconsider Figure 4, where $d = 1.6$. Here we still define influence and pinch-off circles, but because d is not small, the influence circles are larger than the threshold contours. We don't have a microlensing event if the MACHO fails to enter the threshold contour, so in this case we accept only events which pass through the threshold circles (eq. [11]). Then event categorization can be done as before, with trajectory (A) being an offset bright event, trajectory (B) being a merged offset dim event. Trajectory (C) would be classified as borderline, since it is never completely under the influence of only one star. However, it is actually missed by our threshold circle approximation. As discussed in § 4, we are not worried about missing such events since they are very small amplitude (see Fig. 4*b*), and have very little effect on any of our results.

In summary we have introduced several categories of binary microlensing events, which are briefly described in Table 1.

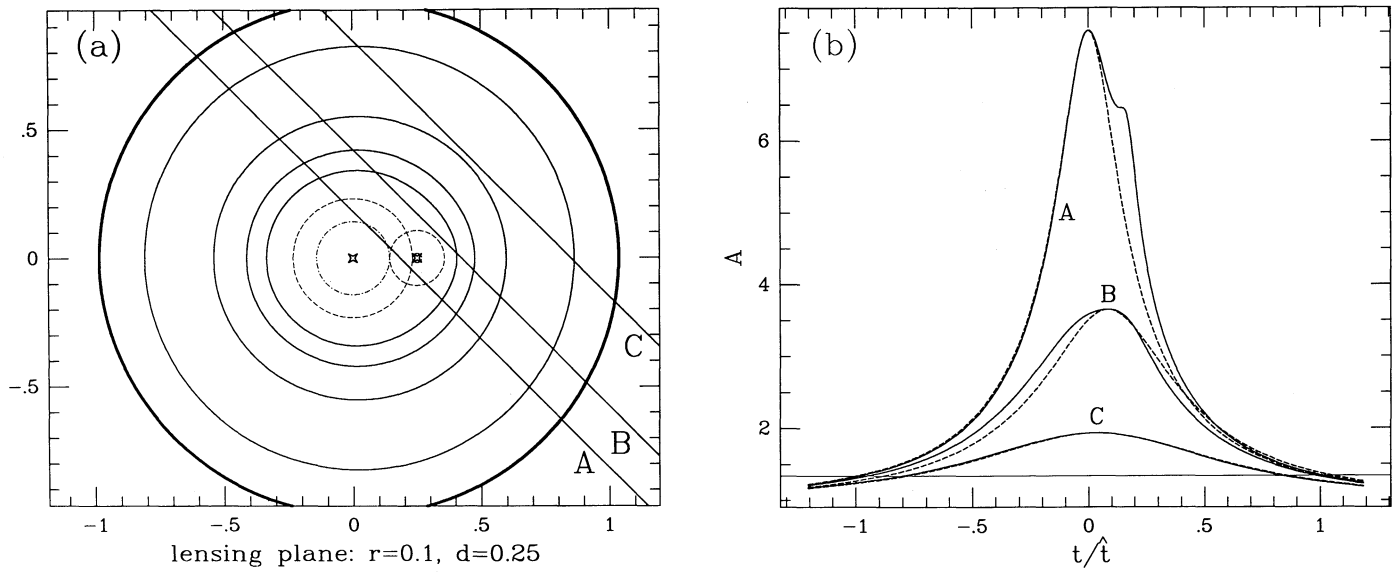

FIG. 6.—Same as Figs. 3 and 4 for $d = 0.25$. Trajectory (A) is an asymmetric, (B) is a borderline, and (C) is an essentially single event.

4. MICROLENSING RATES

Having categorized some of the various types of possible binary microlensing events, we now turn to calculating how often each category of event occurs. We will do this in two stages. First we find the total binary microlensing rate and the relative frequencies of each category of event as a function of the system parameters d, r, and m. Then, in the next section, we average over observational determinations of the distributions of these parameters to find estimates of the expected total rate and expected frequency of each category of event.

To calculate the rate of each category of event we must find the percentage of trajectories which satisfy the criteria for that event category. In general the rate for microlensing is proportional to the rate at which MACHOs enter the microlensing "tube" (or tubes), which is defined as the region of space for which $A > A_T$. (See Griest 1991 for a more complete discussion; especially Figs. 1 and 4.) This rate is proportional to the MACHO speed and the angle averaged threshold radius. Since the microlensing rate for a single source was calculated in Griest (1991), here we will calculate only changes with respect to that assumed known rate. Thus we define the change

$$\eta = \frac{\Gamma_{\rm binary}}{\Gamma_{\rm single}}, \tag{14}$$

where $\Gamma_{\rm single} = C\pi u_T$ and C is a proportionality constant which cancels out in η. (The π comes from the angle average.) Since $R_e \propto m^{1/2}$, and the MACHO density $\rho \propto m^{-1}$, both single source and binary source rates are proportional to $m^{-1/2}$.

When the stars are far apart ($d \gg 1$), then the $A = A_T$ threshold contours are distinct, well separated circles and we expect $\Gamma_{\rm binary} = C\pi(u_{1T} + u_{2T})$, so $\eta \to (u_{1T} + u_{2T})/u_T$ for $d \gg 1$, which is always larger than 1. A plot of this limiting value of η as a function of r for several values of A_T is shown in Figure 7. We see that in general binary stars increase the total microlensing rate between a few and 50%. When the stars are very near each other we expect the total rate to be smaller than that estimated above. In the limit where $d \ll 1$ we expect mainly "effectively single" events and so expect $\eta \to 1$. Note that for realistic observations of the LMC or bulge the secondary stars will not be optically resolved and so these estimates are relevant.

TABLE 1

SUMMARY OF LIGHT CURVE CATEGORIES FOR BINARY SOURCES

Category	Symbol	Criteria	Distinguishable
Offset bright	ob	through only bright star threshold or influence circle	difficult
Offset dim	od	through only dim star threshold circle	possible
Merged offset dim	mod	through only dim star influence circle	yes
Double-peaked	dp	entering both pinch-off circles	yes
Asymmetric	asy	only under influence 1 to only under influence 2, *without* entering both pinch-off circles	yes
Effectively single	es	more than $2d$ away from center of system	no
Borderline	bor	falling between other categories	maybe

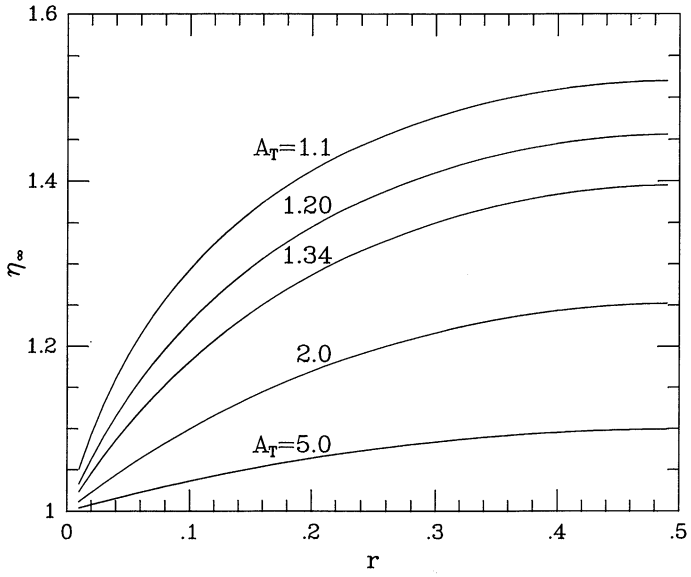

FIG. 7.—Limiting values of $\eta = \Gamma_{\rm binary}/\Gamma_{\rm single}$ (ratio of binary microlensing rate to single source microlensing rate). The stellar separation is taken $d \gg 1$ and η_∞ is plotted as a function of luminosity ratio r for several values of amplification threshold A_T.

For values of d near unity, a more careful analysis is required. When the two threshold circles are distinct, but not far apart, the microlensing rate depends upon the angle of the trajectory. For some angles $d\Gamma_{\rm binary} \propto 2(u_{1T} + u_{2T})$, while if "shadowing" occurs the rate is less. Averaging over all angles we find

$$\Gamma_{\rm binary} \propto 2u_{1T}\theta_s + (u_{1T} + u_{2T})(\pi - \theta_t - \theta_s) - d\,(\cos\theta_t - \cos\theta_s)\,, \quad (d > u_{1T} + u_{2T}) \quad (15)$$

where the shadow angle is

$$\theta_s = \sin^{-1}\,[(u_{1T} - u_{2T})/d]\,,$$

and the tangent angle is

$$\theta_t = \sin^{-1}\,[(u_{1T} + u_{2T})/d]\,.$$

The derivation of equation (15) is given in the Appendix.

When the threshold circles begin to merge ($u_{\rm pinch} < u_T$, or roughly $d \lesssim u_{1T} + u_{2T}$), the calculation of rates becomes more complicated. For the total binary rate we want the angle average of the distance shadowed by the egg-shaped $A = A_T$ contour (see Figs. 4*a* and 5*a*). We calculate this both numerically and by using an approximation which gives reasonable accuracy. The results are shown in Figure 8, where we plot η as a function of d for two values of r. For the approximation we continue to calculate the total rate using two circles, as in equation (15); however, when $u_{\rm pinch} < u_T$, we find the radius of these circles by finding the distance from each star to the closest $A = A_T$ threshold contour. We then use equation (15) with $\theta_t = \pi/2$ to find the total rate through both these circles. This works reasonably well, as shown by the dashed lines in Figure 8. As $d \to 0$ our approximation for η eventually dips slightly below unity, because the actual contours bulge slightly in the direction perpendicular to $\boldsymbol{d}$ (see Fig. 5*a*). As shown in Figure 8, when calculating rates, we will just set η to unity when this occurs. Note that the events we miss by not including this threshold bulge are very low-amplification events which just barely come above threshold (extreme borderline events). Also evident in the numerical determination of the total binary rate is a sharp spike at $d \sim 1.8$–2. As the separate threshold circles merge, a thin "bridge" forms between the circles (see Fig. 4*a*), giving a larger total rate. The trajectories which pass through this bridge (and are therefore missed when we use our circular approximation to calculate the total rates) are very low-amplification events which barely come above threshold, and are neglected (see Fig. 4*b*).

Having found the total binary microlensing rate, we can find the fraction of events which fall into each of the categories defined earlier. When $d > u_{1T} + u_{2T}$ (more precisely $u_{\rm pinch} > u_T$), the rates are easily found. Using the simple formulae in the Appendix, the rate of "offset bright" events (passing only through star 1's threshold circle) and "offset dim" events (passing through only star 2's circle), as well as the fraction of "double-peaked" events (passing through both circles) are (for $u_T < u_{\rm pinch}$):

$$\Gamma_{\rm dp} = C[2u_T\theta_s + (u_{1T} + u_{2T})(\theta_t - \theta_s) + d(\cos\theta_t - \cos\theta_s)]\,,$$
$$\Gamma_{\rm ob} = C\pi u_{1T} - \Gamma_{\rm dp}\,, \quad \Gamma_{\rm od} = C\pi u_{2T} - \Gamma_{\rm dp}\,, \quad (16)$$

where C again is a proportionality constant which cancels out in η. When $u_T > u_{\rm pinch}$ the formulae become more complicated, because we must use the pinch-off and influence circles in addition to the threshold contours. The rate formulae in this case are given in the Appendix.

In order to find the importance of each category of event we use the formulae above and in the Appendix to find the rate at which events satisfying the criteria (defined in § 3 and summarized in Table 1) occur. We then divide this rate by our approximate total rate to find the fraction $f_i(r, d)$ of events in each category i. The rate for "borderline" events is found by subtracting the sum of the rates of all the other categories from the total rate $\Gamma_{\rm binary}$. In Figure 9, we plot these fractions f_i as functions of d for several values of r. The event categories are labeled (see Table 1). The "totd" category is the sum of all "probably distinguishable" events: dp, asy, od, and mod. Note

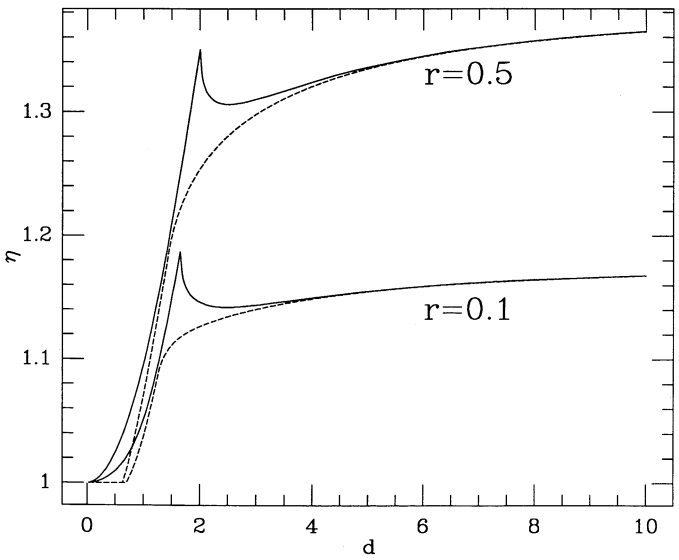

FIG. 8.—Total binary microlensing rate divided by the single source rate, $\eta = \Gamma_{\rm binary}/\Gamma_{\rm single}$ as a function of projected scaled stellar separation d. Values of stellar luminosity offset ratio $r = 0.5$ and 0.1 are shown. The solid lines show the numerical result, and the dashed lines show our approximation.

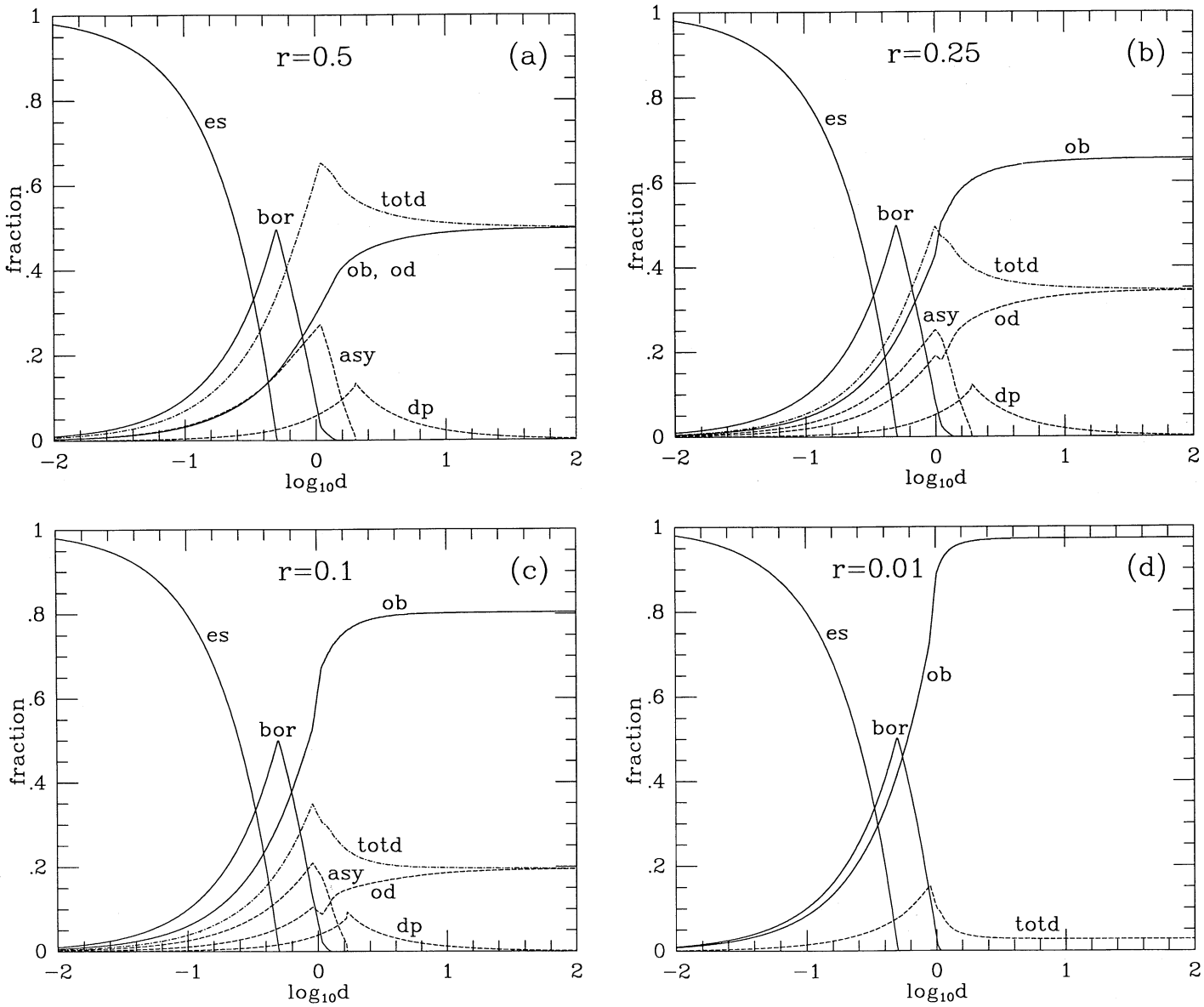

FIG. 9.—Relative importance of various categories of binary microlensing events as a function of projected scaled stellar separation d for several values of luminosity offset ratio r. Part (*a*) shows $r = 0.5$ (equal luminosity stars), while (*b*) shows $r = 0.25$, (*c*) shows $r = 0.1$ and (*d*) shows $r = 0.01$. Curves are labeled by the categories summarized in Table 1: ob: offset bright, od: offset dim (or mod: merged offset dim for small d), asy: asymmetric, dp: double peaked, es: effectively single, and bor: borderline. The dashed lines show the fraction of "probably distinguishable" events (asy + dp + mod + od).

that the abscissa extends from 10^{-2} to 10^{2} Einstein radii. Most of the features in these plots are as expected. For $d \ll 1$ most binary events are "effectively single," and thus have virtually no effect on the microlensing search. For $d \gg 1$ only "offset dim" and "offset bright" events occur with significant probabilities and the ratio of probabilities of offset brights to offset dims is given by $\Gamma_{ob}/\Gamma_{od} \approx u_{1T}/u_{2T} \rightarrow (A_T - 1)u_T/r$ for small r. The regions near $d \sim 1$ are the most interesting. Here probably distinguishable events comprise up to 60% of the total.

The largest percentage of distinguishable events occur near $r = 0.5$ and $d \sim 1$. (For $r = 0.5$ the distinction between offset bright and offset dim is of course meaningless.) As r decreases, the fraction of essentially single and borderline events stays roughly constant, but the fraction of probably distinguishable events drops. At $r = 0.1$, totd peaks at $\sim 35\%$, while by $r = 0.01$ the peak in totd is under 15%. Below $r \sim 0.01$, the number of uniquely binary microlensing events becomes very small—the MACHO is just not very likely to amplify the dim star enough to make a difference.

Having calculated the fraction of events which lie in each category as a function of r and d, and having discussed the detectability of each category of event, we are now ready to make contact with astrophysical observations by averaging our probabilities over realistic distributions in r and d.

5. CONTACT WITH OBSERVATIONS: AVERAGING OVER d, r

In order to apply the results of the previous sections to an actual observing program and predict how large an effect binary sources are expected to produce, we need to know several things. First we need to know the fraction of the observed stars which have companions bright enough to affect a microlensing light curve. Next we need to know, for these

stars, the distribution of separations $\bar{a}$, and the distribution of luminosity offset ratios r. The distribution in $\bar{a}$ can be found (approximately and on average) from the distribution in binary orbital periods P and Kepler's Law, $P^2 = GM_T a^3$, while for main-sequence stars, the r distribution can be found from the distribution in stellar mass ratio $q = M_2/M_1$ (M_1 is the mass of the primary star, M_2 is the mass of the secondary and M_T is the sum), and a mass-luminosity relation.

Since currently planned observation programs are focusing on the LMC or the Galactic bulge, we ideally want the above quantities for stars in the LMC and bulge. In the LMC, given an observational magnitude limit of $\sim$19–20 mag, the observed stars will be mostly K giants and A-B main-sequence stars. For the bulge, most stars will probably be giants, so ideally we want the total binarity and distributions for these populations.

Many studies have been done, and continue to be done, on the total binarity of select samples of stars, and on the period and mass ratio distributions of binaries. For example, Kuiper (1935), Heintz (1969), Abt & Levy (1976), Wolff (1978), Abt & Levy (1978), Abt (1983), Zinnecker (1984), Griffin (1985), Poveda, Allen, & Parrao (1987), Abt & Levy (1985), Halbwachs (1987), Abt, Gomez, & Levy (1990), Trimble (1990), and Duquennoy & Mayor (1991), to name just a few. Unfortunately, a consensus has not been reached, even for the most well studied group of stars in the local solar neighborhood. The problem is that there are several very different methods used to detect binary systems (e.g., visual binary, common proper motion, radial velocities) and each method has severe selection effects which seem to dominate the conclusions (Trimble 1990). However, it is clear that the fraction of stars in binary or multiple systems is very high. Abt (1983) concluded that from studies of radial velocities that somewhere between 50%–100% of normal stars are members of short-period binaries, and from studies of visual companions that nearly 100% of stars are *also* in long-period binaries (for the most part, we will include multiple star systems under the rubric "binary"). In our study, we will leave the total binary frequency as a free parameter, but remember that the normal frequency is probably near unity.

As for the distributions in P and q, our approach will not be to try to find the one best current study or the best fit to all the studies, but to pick three recent and representative studies, selected to span the range of reasonable possibilities. We also will not attempt to use distributions specific to the LMC or bulge, where the data quality is lower, or to focus especially on the somewhat controversial differences in distributions among different types of stars (though in our selection of studies we specifically included two with data from A and B stars). Of these three studies, the best determined distributions are from the Duquennoy & Mayor (1991) study and we use these in generating our primary conclusions. However, we present results for the distributions derived from each of the three studies, the differences arising from use of different distributions perhaps being indicative of the uncertainties in our results.

A careful study of multiplicity of F7–G9 stars in our solar neighborhood has recently been completed by Duquennoy & Mayor (1991, hereafter DM) with much attention being paid to making the sample as unbiased as possible. In a sample of 164 systems they find 62 doubles, seven triples, and two quadruple systems, for a "binary" frequency of 43%, a value rather lower than most. Their distributions in $q = M_2/M_1$ and log P are given in Tables 2 and 3, respectively. We will use the DM distributions even for A and B star primaries since it is the best determined.

Abt and Levy have studied binary systems for decades, and have recently (Abt, Gomez & Levy 1990, hereafter AGL) updated an earlier study (Abt & Levy 1978) of B2–B5 main-sequence stars. After allowing for incompleteness, they conclude that there are 0.8 companions per primary with $q > \frac{1}{4}$, and 1.9 companions per primary with $q > \frac{1}{8}$. Their distributions in q and log P are also given in Tables 2 and 3.

Finally, since many A stars will be observed when LMC stars are monitored for microlensing, we include a study by Abt & Levy (1985, hereafter AL) of A stars. The period distribution for this sample (both Am and A stars) is given in Table 2, and the distribution in q (Am stars only) is given in Table 3.

Other recent determinations of the q distribution have also been given by Trimble (1990), for a sample of mostly K giants, and Halbwachs (1987) for a mixture of types, and could have easily also been considered. However, these studies do not give P distributions and the q distributions fall between the extremes given by the three q distributions discussed above.

From a distribution in $q = M_2/M_1$, the distribution in luminosity offset ratio $r = L_2/(L_1 + L_2)$ can be found for stars on the main sequence using the mass-luminosity relation

TABLE 2

NORMALIZED DISTRIBUTIONS OF $q = M_2/M_1$ FOR BINARY SAMPLES FOR F–G STARS (DM), B STARS (AGL), AND A STARS (AL)

A.

	q			
Distribution	0–0.2	0.2–0.35	0.35–0.7	0.7–1.1
DM (F–G)	25	23	37	15
AGL (B)	39	22	29	10
AL (Am)	6	29	26	39

B.

	q									
Distribution	0–0.1	–0.2	–0.3	–0.4	–0.5	–0.6	–0.7	–0.8	–0.9	0.9–1.1
DM (F–G).....	11	14	16	15	11	12	6	5	3	7

TABLE 3

NORMALIZED DISTRIBUTIONS OF LOG PERIOD FOR BINARY SAMPLES FOR F–G STARS (DM), B STARS (AGL), AND A STARS (AL)

	log P									
Distribution	−1–0	0–1	1–2	2–3	3–4	4–5	5–6	6–7	7–8	8–9	9–10
DM (F–G)	1	4	8	9	13	18	13	14	11	6	3
AGL (B)	...	17	20	4	4	5	7	7	12	24	...
AL (A)	1	10	8	13	13	7	10	22	8	8	...

$L_{ms}/L_{\odot} = (M_{ms}/M_{\odot})^{3.2}$, where because of the larger uncertainties in the distributions, we have not worried about deviations from this approximate relation at high and low masses. In order to turn a period distribution into a distribution in separation, we first use Kepler's law $P^2 = GM_T a^3$ to get a distribution in semi-major axis a, and then follow Duquennoy & Mayor (1991) in using the statistical relation $\log a = \log D + c$, with $c = 0.13$. (Abt & Levy 1978 used the same relation with $c = 0.2$.) Thus, the number of systems N with a scaled projected separation d is

$$\frac{dN}{dd} = \frac{dN}{dP}\frac{dP}{da}\frac{da}{dD}\frac{dD}{dd} = \frac{dN}{dP}\left(\frac{3}{2}M_T^{1/2}a^{1/2}\right)\frac{R_e}{x'}10^{0.13}, \quad (17)$$

where we recall that $D = R_e d/x'$ and we are using $x' = 0.2$ and $L = 50$ kpc throughout [so $R_e/x' \approx 40\ (m/M_{\odot})^{1/2}$ a.u.]. Likewise, the number of systems with luminosity offset ratio r is

$$\frac{dN}{dr} = \frac{dN}{dq}\frac{dq}{dr} \approx \left(\frac{r^{-2}}{3.2}\right)(r^{-1} - 1)^{-4.2/3.2}\frac{dN}{dq}. \quad (18)$$

Given $dN/dddr$ and the probabilities $f_i(d, r)$ of the i categories of microlensing events (i = "ob", "od," "bor," etc.), we can find the total probability of observing a binary light curve of type i

$$P_i = \frac{1}{N}\int_0^{\infty} dd \int_0^{0.5} dr f_i(r, d)\left(\frac{dN}{dddr}\right). \quad (19)$$

Note that we have assumed that the q and P distributions are "factorizable," that is that $dN/dqdP = (dN/dq)(dN/dP)$, and have normalized N to unity. Equation (19) is relevant when using an analytic model of $dN/dqdP$ (which we did initially). However, since the distributions above are binned, we define $n_q = dN/dq$ to be the value of the distribution for the q bins given in Table 2. Likewise we define $n_P = dN/dP$ for the period distributions given in Table 3. Then the probability of a binary event of type i is found by summing over bins.

$$P_i = \sum_{P\text{bins}}\sum_{q\text{bins}} n_P n_q f_i(r_{\text{ave}}, d_{\text{ave}}), \quad (20)$$

TABLE 4

EXPECTED FRACTION OF BINARY EVENTS BY CATEGORY

Mass ($M_{\odot}$)	ob	od	mod	dp + asy	es	bor	totd	$\langle\eta\rangle$
DM (F–G stars) with A0 Primary								
10^{-5}.....	0.78	0.14	0.007	0.015	0.033	0.021	0.16–0.18	1.11
10^{-4}.....	0.74	0.13	0.009	0.017	0.073	0.031	0.16–0.19	1.10
10^{-3}.....	0.69	0.12	0.010	0.021	0.12	0.040	0.15–0.19	1.09
10^{-2}.....	0.62	0.10	0.013	0.028	0.19	0.050	0.14–0.19	1.08
10^{-1}.....	0.53	0.08	0.016	0.032	0.28	0.060	0.13–0.19	1.06
DM with A5 Primary								
10^{-3}.....	0.69	0.12	0.009	0.02	0.12	0.038	0.15–0.19	1.09
10^{-1}.....	0.55	0.079	0.017	0.032	0.26	0.058	0.13–0.19	1.06
DM with B5 Primary								
10^{-3}.....	0.68	0.11	0.011	0.022	0.14	0.040	0.15–0.19	1.09
10^{-1}.....	0.51	0.075	0.015	0.033	0.30	0.066	0.12–0.19	1.06
AGL (B stars) with B5 Primary								
10^{-5}.....	0.68	0.090	0.012	0.027	0.12	0.072	0.13–0.20	1.07
10^{-4}.....	0.59	0.085	0.006	0.014	0.25	0.056	0.11–0.16	1.07
10^{-3}.....	0.55	0.081	0.004	0.009	0.33	0.030	0.09–0.12	1.06
10^{-2}.....	0.51	0.076	0.004	0.009	0.38	0.022	0.09–0.11	1.06
10^{-1}.....	0.48	0.070	0.004	0.010	0.41	0.020	0.08–0.10	1.05
AL (A stars) with A0 Primary								
10^{-5}.....	0.65	0.22	0.014	0.025	0.065	0.030	0.26–0.29	1.17
10^{-4}.....	0.60	0.19	0.021	0.030	0.12	0.037	0.24–0.28	1.15
10^{-3}.....	0.54	0.17	0.020	0.032	0.18	0.052	0.22–0.28	1.13
10^{-2}.....	0.48	0.15	0.016	0.030	0.27	0.054	0.20–0.25	1.11
10^{-1}.....	0.43	0.14	0.014	0.027	0.36	0.040	0.18–0.22	1.10

where we evaluate the distribution f_i at the average value of r in the q bin, $r(q) = (1 + q^{-3.2})^{-1}$. Abt et al. (1990) use four bins for the q distribution: $1 > q > 2^{-1/2}$, $2^{-1/2} < q < 8^{-1/2}$, $8^{-1/2} < q < 32^{-1/2}$, and $32^{-1/2} < q < 128^{-1/2}$, and we bin data into these "course" bins for comparison purposes. The DM study uses finer bins (q between 0 and 1 in steps of 0.1) so when using this data set alone we will use these finer bins. The difference in results between using the course and fine bins is not great. Because f_i changes rapidly with d, we actually performed the integral over P approximately using the binned values.

The results of this averaging for each of the three different data sets are shown in Table 4 which constitutes a main result of this paper.

The results shown in Table 4 show the division into categories for a sample of stars of a given type, for a given MACHO mass and for the given P and q distributions. Because of the steepness of the mass-luminosity relation, the results depend somewhat on the luminosity of the primary star, though as seen from the entries labeled DM with A0 primary, A5 primary, and B5 primary, the differences are small. The symbols such as "ob," "dp,", etc., are defined in Table 1. The column in Table 4 labeled "totd" is, in some sense, the bottom line of this paper. This is the total fraction of binary microlensing events which we expect to be probably distinguishable from single source microlensing events. It includes "od" + "mod" + "dp" + "asy" and perhaps "bor" events. The range in "totd" values listed in Table 4 come from whether or not borderline events are included as probably distinguishable from single source events. The "totd" events are the ones which might be rejected as due to nonmicrolensing causes if care is not taken. We have a total fraction of distinguishable events between 10% and 20%. We now discuss these results in more detail.

Examination of the P and q distributions (Tables 2 and 3) show very large variations among them, and these variations are reflected in the factor of 2 or more differences between corresponding entries in Table 4. For the most part the results in Table 4 can be understood from the distributions in Tables 2 and 3, and the results shown in Figure 9. For example, the ratio of offset bright to offset dim events is inversely proportional to the "average" value of r. Since the AGL(B star) distribution peaks at low values of r, we see it has a larger ob/od ratio than the DM(F–G star) distribution, which in turn has a larger ratio than the AL(A star) distribution which peaks at large values of r.

Figure 9 shows that the switch over from essentially single events to offset bright and offset dim events occurs for $d \sim 10^{-0.5}$–$10^{0.5}$, and that in this range the most uniquely binary light curves (dp, asy, mod) occur. Using $P = M_T^{1/2}(10^{0.13} R_e\, d/x')^{3/2}$, this d range corresponds to periods in the range

$$P \approx (10^4 - 10^6)(m/M_\odot)^{3/4} \text{ days} . \quad (21)$$

When one of the high-valued bins in a period distribution falls in this range, we expect a large contribution to the double-peaked, asymmetric, and merged offset dim categories. Examination of Table 4 bears this out.

The bins with periods below the range given in equation (21) contribute mostly to effectively single events, and so for example with $m = 10^{-5}\, M_\odot$, we expect from Table 3, twice as many AGL(B star) effectively single events as AL(A star) "es" events, and 4 times as many as from the DM(A–F star) distribution. This is just what is found in Table 4. The bins with periods longer than the equation (21) range above contribute mostly to offset bright and offset dim events as expected.

Thus we see the contributions from the various categories. The fraction of offset bright events ranges from 65%–78% at $m = 10^{-5}\, M_\odot$ to 43%–53% at $m = 10^{-1}\, M_\odot$. The fraction of separated offset dim events varies from between 8% and 22%, while the fraction of merged offset dim events varies from 0.4% to 2%. Double-peaked plus asymmetric events comprise from less than 1% to around 3% of the total, while essentially single events comprise between 3% and 40% depending upon the MACHO mass and distribution used. Borderline events give between 2% and 7% of the total. Including the variation from all three distributions, the total percentage of probably distinguishable events ranges from 8% to 29%, with the more well-determined DM distribution giving a 13%–19% range.

In summary, the fraction of uniquely binary light curves (dp, asy, and mod) is actually quite small, less than 5% in all cases. We see that our initial worry that most binary light curves might be rejected as microlensing candidates is not borne out. While a measurable fraction of binary light curves will be uniquely binary, the large majority will not differ greatly from single source light curves, even assuming 100% of observed stars are members of binary systems. However, for the 10%–20% (DM and AGL distributions) of binary light curves which are probably distinguishable from single source light curves, care should be taken so as not to reject them from the microlensing candidate pool. It would be quite interesting and worthwhile to see examples of such light curves. (For example, information concerning the MACHO velocity could be extracted.)

Finally, we should note that for the most part, we have not considered binaries in which giant stars are the primary (see the sections on achromaticity and binary motion for exceptions), even though a large fraction of LMC stars and most Galactic bulge stars observed are expected to be giants. The main reason is that we do not, for the most part, expect the companion to be bright enough to cause the various effects discussed. Unless luminosity ratio r is larger than ~ 0.01, the chance of significant effect on the light curve is small. At the LMC distance the bulk of the observed stars will be A, B, and giant stars. A giant star formed from an F–K type main-sequence star is unlikely to have an A or B star companion, since the A and B lifetimes are shorter than the F–K main-sequence times.

Imagine a main-sequence binary. The more massive and therefore brighter star will evolve into a giant first, becoming 30–1000 times brighter and decreasing r by this factor. Thus we expect a giant main-sequence binary system to have $r < 0.03$, and typically, $r < 0.01$. It is possible for both stars to enter simultaneously the giant phase, but this requires that their masses to be very nearly equal. Since stars spend more than 90% of their lives on the main sequence, the binary members' main-sequence lifetimes τ, would have to be equal to within 10% for both stars to coexist in the giant phase. Using $\tau \propto M^{-2.2}$, with $\Delta\tau/\tau < 0.1$, would require $\Delta M/M < 0.1/2.2$, i.e., that the masses be equal to within $\sim 5\%$. The Duquennoy & Mayor (1990) distribution of binary masses shows that fewer than 3% of binaries have masses within 10% of each other. Since low-mass stars spend more time on the giant branch and the mass-luminosity relation steepens as mass decreases, a more realistic estimate would give even fewer simultaneous giant binaries. Thus we do not expect many double giant stars. We should note that this argument does not apply to Algol

type systems, where a main-sequence star is in a contact binary with a giant star. Mass loss/transfer is suspected to be involved here, and we will not consider microlensing of this class of binaries. Finally, we should note that for smaller mass MACHOs the light curve from a giant star source is not given by the pointlike star approximation, given in § 2. Thus, in general, giant stars should be treated separately. In summary, we have presented results only for main-sequence stars, primarily because more of these binaries will have $r > 0.01$.

6. COLOR SHIFT LIGHT CURVE

Achromaticity is an important signature of a true microlensing light curve. However, as pointed out by Spiro (1990), if only one component of a binary source is lensed, the event will not be achromatic. The formalism for calculation of the expected shift in color was discussed in § 2. Here we apply it in conjunction with the empirical distributions in q and P.

First recall that when discussing color shifts, luminosity offset ratios in both color bands are required (r_V and r_B for example, see eq. [8]). Previously we used the mass ratio q and a mass-luminosity relation to derive $r = L_2/(L_1 + L_2)$ in some color band. In order to calculate a color shift light curve we also require the color, or equivalently the M–K classification of the stars.

As an example, consider a K0/A0 binary with M_V magnitudes of 0.6/0.7 and M_B magnitudes of 1.63/0.7, respectively. Note that we are considering a giant/main-sequence binary here, even though we just argued that such cases should be rare. We use this as an illustration because the color shifting is large in such a case. When we estimate the expected size of a typical color shift, we will return to exclusively main-sequence binaries.

Using equation (6) we find $r_V = 0.523$ and $r_B = 0.298$. Thus the formula for the color shift light curve is $A_{B-V} = (0.477A_1 + 0.523A_2)/(0.702A_1 + 0.298A_2)$, where A_1 and A_2 are the amplifications from the K0 giant and A0 star respectively (eq. [1]). All possible color shift light curves for this system can be shown in A_{B-V} [or equivalently $\Delta(B-V)$] contour diagrams, such as Figure 10. Figure 10*a* shows two stars (A0 on left and K0 on right) separated (in the lensing plane) by $d = 0.7$. As the MACHO moves through this plane it will cross various contours of constant $\Delta(B-V)$ (labeled in the figure). For example, if a MACHO crosses a contour labeled 0.1, at that time the apparent $B-V$ of the system will be 0.1 mag higher than before the microlensing event took place. A MACHO trajectory through this plane thus generates a $\Delta(B-V)$ light curve, such as shown in Figure 10*b*. We see that in the regions between the stars the color shift is near zero, but as the MACHO approaches either star, $\Delta(B-V)$ increases in absolute value, tending towards the limiting values

$$A_{B-V}(\text{star 1 lim}) \rightarrow \frac{1-r_V}{1-r_B}, \quad A_{B-V}(\text{star 2 lim}) \rightarrow \frac{r_V}{r_B}, \quad (22)$$

where $\Delta(B-V) = 2.5 \log A_{B-V}$. For our example $\Delta(B-V) \rightarrow -0.42$ mag near to the A0 star and $\Delta(B-V) \rightarrow 0.61$ mag near to the K0 star. Note for comparison that a classical Cepheid with a 10 day period has a min/max shift in $B-V$ of 0.43 mag, while an RR Lyrae with a 1 day period has $\Delta(B-V) \sim 0.25$ (Allen 1973).

Also note that if a well-measured color shift light curve of the type shown in Figure 10*b* were obtained, the trajectory of the MACHO (in the scaled lensing plane) could be determined apart from a two-fold ambiguity arising from the reflection symmetry in the geometry. When $\Delta(B-V)$ is at its maximum, the trajectory is tangent to the $\Delta(B-V)$(max) contour, while when $\Delta(B-V) < 0$ is at its minimum, the trajectory must be tangent to the minimum contour. Examination of Figure 10*a* shows only two pairs of trajectories which satisfy both constraints; of which only one pair would generate the observed light curve. A similar procedure could also be applied to a double-peaked light curve, even if no color shift light curves were obtained.

The color shift light curve caused by trajectory (A), shown in

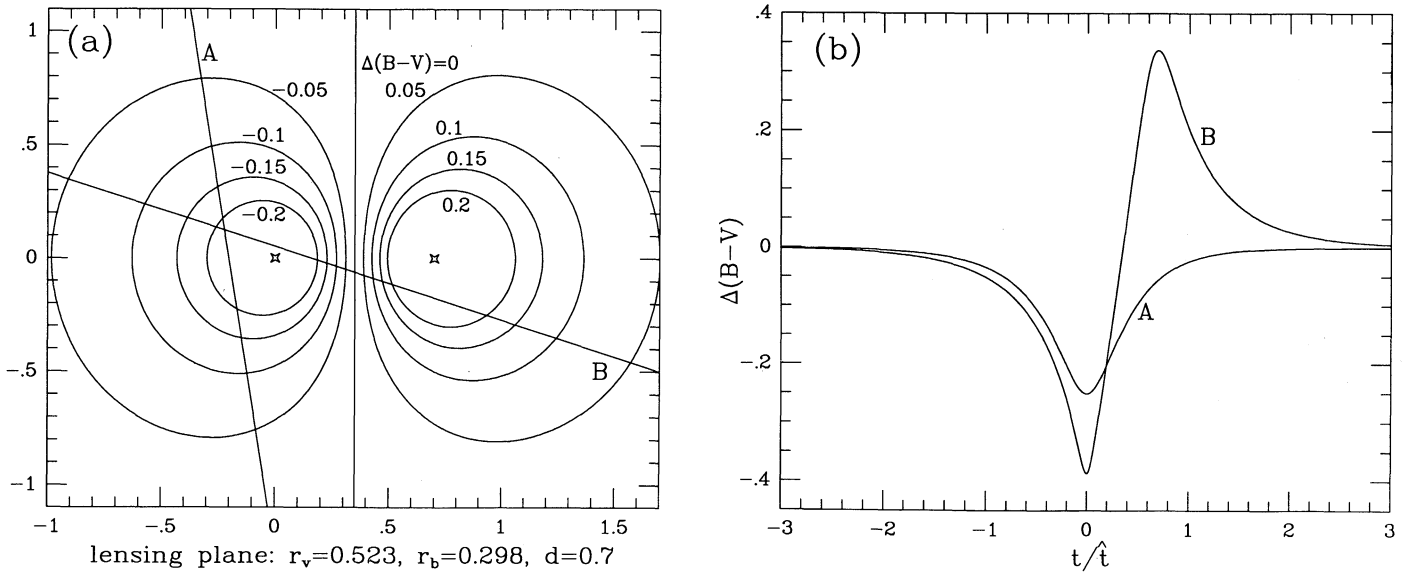

FIG. 10.—Contour plots of $\Delta(B-V)$, MACHO trajectories, and the resulting color shift light curves for binary sources. Part (*a*) shows contours of $\Delta(B-V)$ in the lensing plane for $d = 0.70$, $r_V = 0.523$, and $r_B = 0.298$ (A0 and K0 stars). Contour values are labeled. Two MACHO trajectories are also labeled (A) and (B) (*straight solid lines*). Part (*b*) shows the color shift light curves resulting from the labeled trajectories.

Figure 10*b* is quite distinctive and quite different from a typical variable star color shift light curve. A curve which results from a trajectory such as (B), however, might be confused with a new type of variable star and the microlensing event might be rejected as a microlensing candidate. (Again, a poorly programmed computer might also reject curves from trajectories of type A.)

Now, as we mentioned, we do not expect many K0/A0 binary systems due to the mismatch in giant and main-sequence lifetimes. A more likely combination is a pair of main-sequence stars such as A0/F5. Using $M_V = 3.3$ and $M_B = 3.77$ for the F5 (Allen 1973) we find $r_V = 0.084$ and $r_B = 0.058$. Now the limiting values become $\Delta(B-V)_{\max} = 0.040$ and $\Delta(B-V)_{\min} = -0.30$, giving a much smaller signal. This is to be expected, since for two main-sequence stars, either they have nearly the same color (if they are close in mass), or one star is much dimmer (if they are quite different in mass). In either case, we do not expect very large color shifting to occur.

In order to quantify the expected color shift, we can average over one of the observed distributions [DM(A–F)] discussed in § 5. We consider three different primary stars: A0, A5, and B5 and average over all fainter main-sequence secondaries. We find the fraction of events which give a maximum $\Delta(B-V)$ greater than 0.1 mag. For an A0 primary star and MACHO mass $m = 10^{-3}\ M_\odot$, we find $\sim$2.9% of events will have a maximum $\Delta(B-V)$ of greater than 0.1 mag. For A5 and B5 stars, the fractions are 3.7% and 1.7%, respectively. For an A0 primary and $m = 10^{-5}\ M_\odot$, the fraction is 4.4%, while for an A0 with $m = 10^{-1}\ M_\odot$ it is 2.4%. These numbers were found very approximately, without a careful search of merged threshold events and we estimate them to be accurate only to within a factor of 2. The differences between the DM, AGL, and AL period distributions give an unavoidable uncertainty that is this large in any case. (We used the DM distribution for the above numbers.) Note that for $r \gtrsim 0.1$, it may be possible to spectroscopically distinguish between binary and single stars.

The shifts are quite small compared to an estimated MACHO collaboration photometric accuracy of 5%–10%. However, for larger MACHO masses where many measurements will be made on a typical light curve, the color shift should be a measurable effect. Our original worry, however, that many true microlensing events might be rejected because of achromaticity, seems unlikely to occur.

7. MISESTIMATING THE MACHO MASS

In this section we briefly consider the misestimation of underlying MACHO parameters which may occur if binary microlensing is not taken into account. First recall that for a single source microlensing event, the simple relationship $u_T^2 = u_{\min}^2 + (t_e/\hat{t})^2/4$ holds, where the threshold u_T is set by the observer, $u_{\min}$ is determined from the maximum amplification, t_e is the measured event duration, and $\hat{t} = R_e/v_\perp$ contains the MACHO parameters ($R_e \propto m^{1/2}$). For arguments sake, suppose that the MACHO distance and transverse velocity are known. Then measurement of $u_{\min}$ and t_e result in a determination of the MACHO mass. For large amplification events, $u_{\min}$ is small and $\hat{t} \approx t_e/2u_T \propto m^{1/2}$.

When binary sources are involved, both minimum distances $u_{\min 1}$ and $u_{\min 2}$ are needed, as is the scaled projected stellar separation $\boldsymbol{d}$ (see Fig. 2). Because various types of microlensing light curves can occur, no one simple formula relates the event duration to the MACHO mass. When the light curve is clearly the result of binary microlensing, one should fit for the various parameters and use the full formula, equation (4). However, there are some estimates which can be made in general. For example, since the *average* event duration is the optical depth to microlensing divided by the total microlensing rate, an expected average shift in event duration can be calculated. The expected mistake in estimating MACHO mass can be estimated from this. In addition, for certain categories of binary events, such as offset bright and offset dim, the formulae simplify and estimates of the misestimation of MACHO mass can be made.

Consider first a large amplification offset bright event, where effectively only the bright star is lensed. As shown in § 3, this type of event is difficult to distinguish from a single source event and hence an estimate of the MACHO mass is likely to be made using the single source formula. The duration of the event is, as always, the time for which $A > A_T$, and we suppose that, in this case, we can ignore the amplification of the faint star ($A_2 = 1$). The duration condition becomes $A_1 > A_{1T}$, where A_{1T} is given in equation (11). For small $u_{\min}$, the ratio of the actual value of $\hat{t}$ to the $\hat{t}$ one would get using the single source assumption is u_T/u_{1T}. The actual MACHO mass would be larger than the single source formula mass by a factor $(m_{\rm true}/m_{\rm sing})_{\rm ob} = (u_T/u_{1T})^2$ (assuming x' and $v_\perp$ were known). This ratio is plotted as a function of r in Figure 11 (*dashed line*). Note that this is a very approximate result since we set $u_{\min 1} = 0$ and did not consider the amplification of star 2. However, it does show that one might expect an error of up to a factor of 2 for offset bright events.

A similar expression holds for large amplification offset dim events, where only the dim star is lensed. Making the same approximations as before gives $(m_{\rm true}/m_{\rm sing})_{\rm od} = (u_T/u_{2T})^2$, which is a much larger effect, plotted in Figure 11 (*dashed line*). For $A_T = 1.34$ and small r, $(m_{\rm true}/m_{\rm sing})_{\rm od} \approx (A_T - 1)^2 r^{-2}$. During offset dim events most of the amplification is drowned in the light of the brighter star, giving only a very short observable peak as the MACHO comes very close to the dim star.

The dashed lines in Figure 11 show that the mass mis-

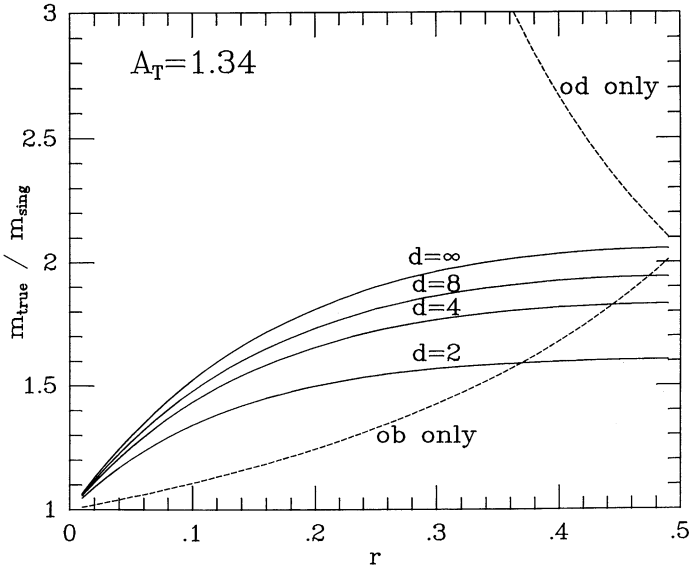

FIG. 11.—Misestimates of MACHO mass if single source formulas are used. The dashed lines show the misestimation ratio for offset bright (ob) and offset dim (od) events. The solid lines show the misestimation averaged over all event types for $d = 2, 4, 8$, and ∞.

estimation for offset bright and offset dim events depends sensitively on r. We can find the expected misestimation for these events types by averaging over the three q and P distributions discussed in § 5. For the DM(F)–(G) distribution, $\langle m_{\rm true}/m_{\rm sing}\rangle = 1.05$ for offset bright events and it is 5.3 for offset dim events. For the AL(A) distributions the numbers are 1.04 and 7.3, respectively, while for the AGL(B) distributions they are 1.1 and 3.2, respectively. Recall that we expect to be able to distinguish offset dim events by the light curve shape, so hopefully one would not use the single source fomula in deriving the MACHO mass. If one did, however, the error would be substantial. Offset bright events, however, are probably indistinguishable, so a 5%–10% error in mass estimation may be unavoidable for these events (which constitute a large fraction of the total). It may, however, be possible to check for duplicity spectroscopically.

Finally, the dashed lines in Figure 11 give the misestimation of mass for only a special class of events. More generally, perhaps, one would like to average over all types of events to find an expected miscalculation of MACHO mass. In practice, the MACHO mass will be found using the method of moments (DeRujula, Jetzer, & Masso 1990), or maximum-likelihood fitting, so finding the precise miscalculation in the binary case is beyond the scope of this paper. However, an estimate can be made as follows. As described in Griest (1990), the average or expected event duration is $\langle t_e\rangle = \tau/\Gamma_{\rm tot}$, where the optical depth τ is the total number of MACHOs inside the microlensing tube (proportional to the total area of the $A = A_T$ contour), and the total rate $\Gamma_{\rm tot}$ is the rate at which MACHOs enter the tube (proportional to the angle averaged cross-sectional area). Using our calculation of binary rates, etc., we can therefore find $\langle t_e\rangle_{\rm binary}$ and $\langle t_e\rangle_{\rm sing}$. We expect approximately $\hat{t}_{\rm sing}/\hat{t}_{\rm binary} = \langle t_e\rangle_{\rm sing}/\langle t_e\rangle_{\rm binary}$, so can estimate $\langle m_{\rm true}/m_{\rm sing}\rangle \approx (\langle t_e\rangle_{\rm sing}/\langle t_e\rangle_{\rm binary})^2$. For binary stars far from each other ($d \gg 1$), $\tau \propto u_{1T}^2 + u_{2T}^2$, and $\Gamma_{\rm tot} \propto u_{1T} + u_{2T}$. Thus in the large d limit we have

$$\left\langle \frac{m_{\rm true}}{m_{\rm sing}} \right\rangle_{d=\infty} \approx \left[\frac{u_T(u_{1T} + u_{2T})}{u_{1T}^2 + u_{2T}^2} \right]^2 . \tag{23}$$

A plot of equation (23) is given in Figure 11 (labeled $d = \infty$).

However, equation (23) assumed that $d \gg 1$. For other values of d we can use the more general event rate formulae discussed in § 4. The result then becomes dependent upon the value of d. We plot the mass misestimation ratio for several values of d in Figure 11. We did not consider d near unity where calculation of the rate and optical depth becomes more tedious. The solid lines in Figure 11, however, do not represent the actual mistake one would make since, hopefully, single source formulae would not be used for distinguishable events.

In summary, we find a significant misestimation of MACHO mass when the binary nature of the source is not taken into account. For events in which distinguishability is difficult (offset bright events) we expect to estimate the mass small by up to a factor of 2 (but 5%–10% on average). For offset dim events the mass estimate can be off by orders of magnitude, but here one hopes to be able to recognize the binary nature of the event and take it into account. On average, for binary microlensing, if no account is taken of binarity, the mass will be misestimated by between a very small amount and a factor of 2 depending upon d and r.

8. BINARY MOTION

In this section we very briefly discuss another physical mechanism in binary systems which can affect microlensing. In a binary system, both stars orbit their common center of mass so as the orbit proceeds the lines of sight to the observer vary. Thus the usual assumption that the MACHO has a straight-line trajectory is not valid. Depending upon the size and period of the orbit, the size and position of the Einstein ring, and the MACHO velocity, this can be a negligible or observable effect.[5] If the duration of the microlensing event is long compared to the binary period, then small "ripples" will appear on the light curve as illustrated in Figure 12. Various other light curve distortions will result if the binary period is comparable to the event duration.

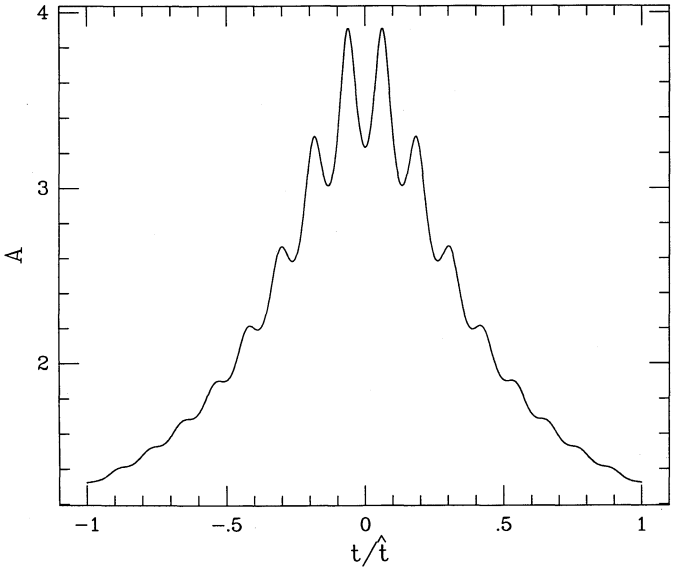

FIG. 12.—Binary microlensing light curve where orbital motion is important (see text).

Note, however, that light curves such as that shown in Figure 12 are extremely unlikely. In order to have such an event, the projected binary semi-major axis must be comparable in size to the Einstein ring radius ($d \sim 1$). The orbital period must also be comparable to the event duration, $\hat{t} \sim P$ [or $(GM_T)^{1/2}D^{3/2} \sim R_e/v_\perp$]. For LMC observations there is no natural range of parameters which simultaneously satisfy both of these constraints. For example, for $M_T = 3\ M_\odot$, $x' = 0.2$, $L = 50$ kpc, the second constraint becomes $v_\perp \sim 0.09m^{-1/4}d^{-3/2}$ km s^{-1}, requiring an unusually low value of $v_\perp$ for reasonable MACHO mass. To generate Figure 12, we assumed a circular face-on orbit with $P = 100$ days, $m = 10^{-5}\ M_\odot$, $u_{\rm min} = 0.3$, $r = 0.5$, and $v_\perp = 1$ km s^{-1}. This gives $\hat{t} = 441$ days and $d = 0.23$. All these parameters are reasonable except $v_\perp$, which typically would be $\sim$200 km s^{-1} for halo dark matter MACHOs. For parameters consistent with more reasonable values of $v_\perp$ the amplitude of the ripples is very small or the event duration is too short for the effect to be significant. Thus we do not expect many cases such as shown in Figure 12 to be detected.

We would like to thank Andy Gould for many helpful suggestions.

[5] Andy Gould (1992) has independently discussed this effect, only using the Earth's motion around the Sun instead of the binary motion. For $x' = 0.2$, the effect of the Earth's motion will be larger than that of binary motion (for the same D and P) by a factor $(1 - x')/x'$.

APPENDIX

BINARY EVENT RATES

A1. TOTAL RATE APPROXIMATION

The total microlensing rate is proportional to the probability that a trajectory takes the MACHO within the given threshold. The separation $d_{\rm crit}$ at which $A_{\rm pinch} = A_T$ is the dividing line between a merged and a separate threshold contour. At separations several times greater than $d_{\rm crit}$, the threshold is given approximately by two circles whose radii can be well approximated by considering the contribution of the companion as background:

$$A_{1T} = (A_T - r)/(1 - r)\,, \qquad A_{2T} = (A_T + r - 1)/r\,. \tag{A1}$$

When $d_{\rm crit} < d$, we may extend this formalism by finding numerically the threshold on the stellar axis. Taking the distance to the nearer star as radius, we then approximate the contour by two overlapping circles. Note that in this limit the threshold circles will form a merged overall threshold contour. At a given angle the rate of lensing events is proportional to the one-dimensional cross section presented by the threshold contour. Since there is symmetry with respect to the stellar axis and time reversal, we need only consider angles in a single quadrant. There are two important angles, $\theta_t = \sin^{-1}[(u_{1T} + u_{2T})/d]$ above which the projections do not overlap, and $\theta_s = \sin^{-1}[(u_{1T} - u_{2T})/d]$, below which the projection of the bright star completely shadows that of the dim. Simple geometry gives us that the total rate is proportional to

$$\begin{aligned} d\Gamma_{\rm binary} &\propto 2u_{1T}\,d\theta && 0 < \theta < \theta_s\,,\\ d\Gamma_{\rm binary} &\propto [(u_{1T} + u_{2T}) + d\,\sin\,\theta]d\theta && \theta_s < \theta < \theta_t\,,\\ d\Gamma_{\rm binary} &\propto 2(u_{1T} + u_{2T})d\theta && \theta_t < \theta < \pi/2\,. \end{aligned}$$

Since all angles are equally likely, the total rate of microlensing is given by integrating this equation yielding

$$\Gamma_{\rm binary} = C[2u_{1T}\theta_s + (u_{1T} + u_{2T})(\pi - \theta_t - \theta_s) - d(\cos\,\theta_t - \cos\,\theta_s)]\,, \tag{A2}$$

where C is a proportionality constant which cancels out since we only report the relative increase in the microlensing rate

$$\eta = \Gamma_{\rm binary}/\Gamma_{\rm sing}\,, \tag{A3}$$

where $C\pi u_T$ is the rate of single source lensing. In reality, this ratio is always greater than one. The circular approximation breaks down at small separation (see Fig. 8). In practice, therefore, when $\Gamma_{\rm binary}$ calculated above becomes less than $C\pi u_T$, we have replaced it with $\Gamma_{\rm binary} = C\pi u_T$.

A2. EVENT CATEGORIZATION

The separation $d_{\rm crit}$ also divides the events into two broad categories. For distances $d > d_{\rm crit}$, we have the independent threshold events: offset bright (ob), offset dim (od), and double-peaked (dp). For $d < d_{\rm crit}$, merged threshold events are obtained: offset bright (ob), merged offset dim (mod), double-peaked (dp), asymmetric (asy), essentially single (es), and borderline (bor).

Independent threshold offset events will occur when $d > d_{\rm crit}$ and the MACHO passes through the threshold of one and not the other. Offset bright events occur when the MACHO passes through the threshold of the brighter star, offset dim, through that of the dim star. Events that occur by passing through both thresholds are double-peaked events.

The rate of double-peaked events may easily be found to be proportional to

$$\begin{aligned} d\Gamma_{\rm dp} &\propto 2u_{2T}\,d\theta && 0 < \theta < \theta_s\,,\\ d\Gamma_{\rm dp} &\propto [(u_{1T} + u_{2T}) - d\,\sin\,\theta]d\theta && \theta_s < \theta < \theta_t\,,\\ d\Gamma_{\rm dp} &\propto 0 && \theta_t < \theta < \pi/2\,. \end{aligned}$$

Thus

$$\Gamma_{\rm dp} = C[2u_{2T}\theta_s + (u_{1T} + u_{2T})(\theta_t - \theta_s) + d(\cos\,\theta_t - \cos\,\theta_s)]\,, \qquad \Gamma_{\rm ob} = C\pi u_{1T} - \Gamma_{\rm dp}\,, \qquad \Gamma_{\rm od} = C\pi u_{2T} - \Gamma_{\rm dp}\,, \tag{A4}$$

where C is a proportionality constant. Division by the total rate $\Gamma_{\rm binary}$ yields the relative probabilities of the various types.

There is a natural extension of these categories when $d < d_{\rm crit}$. Although the threshold tubes are already merged, and thus every event is influenced somewhat by both stars, we may define regions of relative influence of the two stars. There will always exist an amplification and corresponding distance at which the contour separates into two distinct tubes. We have defined this in the text as $A_{\rm pinch}$. Corresponding to equation (A1), we may approximate this contour with circles whose radii, caled $u_{1\,\rm pin}$ and $u_{2\,\rm pin}$, are given by considering the second star as background. These circles define a region within which the influence of the other star can be effectively ignored. Double-peaked events can be obtained by the MACHO passing through both of these regions. Correspondingly, the rate of such events, $\Gamma_{\rm dp}$, is given by the equation (A4) above with the substitution of $u_{1\,\rm pin}$ for u_{1T} and $u_{2\,\rm pin}$ for u_{2T}.

The region of strong influence of each star, within which it has the ability to distort significantly the light curve, extends to a greater region however. On the axis, it extends to the point at which its companion becomes completely dominant, i.e., the pinch-off circle of the companion. Therefore we define two influence circles $u_{1\,\rm inf} = d - u_{2\,\rm pin}$ and $u_{2\,\rm inf} = d - u_{1\,\rm pin}$. Asymmetric single-peaked and double-peaked light curves can be obtained by passing through the region solely under the influence of one star to the region

solely under the influence of the other. Trajectories that pass between the stars where the influence circles overlap are equally influenced and result in symmetric curves. These are classed as borderline cases. Offset bright events in the merged threshold case are defined as all those whose trajectories take the MACHO through the influence circle of the brighter and not that of the dimmer. Since the resulting light curves are similar to the independent threshold offset bright curves, we will not consider the two categories separately. Merged offset dim are the extension of offset dim events and consist of events which go through the influence circle of the dimmer and not the brighter. Merged offset dim light curves differ from offset dim curves in that they have a broad shoulder due to the influence of the brighter star. The rates for the merged offset events are calculated as above by replacing threshold circles with influence circles. Note that the influence circles may only replace the threshold circles when they individually come within the threshold.

Now let us quantify this description and calculate the rate of merged threshold events. We must introduce two additional tangent angles:

$$\alpha = \cos^{-1}\left[(d^2 + u_{1\,\mathrm{inf}}^2 - u_{2\,\mathrm{inf}}^2)/(2u_{1\,\mathrm{inf}}\,d)\right], \qquad \beta = \cos^{-1}\left[(d^2 + u_{2\,\mathrm{inf}}^2 - u_{1\,\mathrm{inf}}^2)/(2u_{2\,\mathrm{inf}}\,d)\right],$$
$$\theta_{t1} = \pi/2 - \beta, \qquad \theta_{t2} = \pi/2 - \alpha. \tag{A5}$$

If P_0 is the point of intersection of the two influence circles, P_1 is the position of star 1 and P_2 is the position of star 2, then α is the angle between P_1P_2 and P_1P_0, and β is the angle between P_2P_1 and P_2P_0. The shadow angle θ_s' is again important as well:

$$\theta_s' = \sin^{-1}\left[(u_{1\,\mathrm{inf}} - u_{2\,\mathrm{inf}})/d\right]. \tag{A6}$$

If $\theta_s' < \theta_{t1}$, then geometry tells us

$$\begin{aligned}
d\Gamma_{\mathrm{dp+asy}} &\propto 2u_{2\,\mathrm{inf}}\,d\theta && 0 < \theta < \theta_s',\\
d\Gamma_{\mathrm{dp+asy}} &\propto (u_{1\,\mathrm{inf}} + u_{2\,\mathrm{inf}} - d\,\sin\theta)d\theta && \theta_s' < \theta < \theta_{t1},\\
d\Gamma_{\mathrm{dp+asy}} &\propto [u_{1\,\mathrm{inf}}\,\sin\alpha\,\cos\theta + u_{1\,\mathrm{inf}} - (d - u_{2\,\mathrm{inf}}\,\cos\beta)\,\sin\theta]d\theta && \theta_{t1} < \theta < \theta_{t2},\\
d\Gamma_{\mathrm{dp+asy}} &\propto 2u_{1\,\mathrm{inf}}\,\sin\alpha\,\cos\theta\,d\theta && \theta_{t2} < \theta < \pi/2.
\end{aligned}$$

We find

$$\Gamma_{\mathrm{dp+asy}} \propto 2u_{2\,\mathrm{inf}}\,\theta_s' + (u_{1\,\mathrm{inf}} + u_{2\,\mathrm{inf}})(\theta_{t1} - \theta_s') + d(\cos\theta_{t2} - \cos\theta_s') + u_{1\,\mathrm{inf}}(\theta_{t1} - \theta_{t2})$$
$$- u_{2\,\mathrm{inf}}\,\cos\beta(\cos\theta_{t2} - \cos\theta_{t1}) - u_{1\,\mathrm{inf}}\,\sin\alpha(\sin\theta_{t2} + \sin\theta_{t1} - 2).$$

Whereas if $\theta_s' > \theta_{t1}$

$$\begin{aligned}
d\Gamma_{\mathrm{dp+asy}} &\propto 2u_{2\,\mathrm{inf}}\,d\theta && 0 < \theta < \theta_{tl},\\
d\Gamma_{\mathrm{dp+asy}} &\propto [u_{2\,\mathrm{inf}}\,\sin(\theta + \beta) + u_{2\,\mathrm{inf}}]d\theta && \theta_{t1} < \theta < \theta_s',\\
d\Gamma_{\mathrm{dp+asy}} &\propto [u_{1\,\mathrm{inf}}\,\sin\alpha\,\cos\theta + u_{1\,\mathrm{inf}} - (d - u_{2\,\mathrm{inf}}\,\cos\beta)\,\sin\theta]d\theta && \theta_s' < \theta < \theta_{t2},\\
d\Gamma_{\mathrm{dp+asy}} &\propto 2u_{1\,\mathrm{inf}}\,\sin\alpha\,\cos\theta\,d\theta && \theta_{t2} < \theta < \pi/2,
\end{aligned}$$

and we find

$$\Gamma_{\mathrm{dp+asy}} \propto u_{2\,\mathrm{inf}}(\theta_{t1} + \theta_s') - u_{2\,\mathrm{inf}}[\cos(\theta_s' + \beta) - \cos(\theta_{t1} + \beta)] + (d - u_{2\,\mathrm{inf}}\,\cos\beta)(\cos\theta_{t2} - \cos\theta_s')$$
$$+ u_{1\,\mathrm{inf}}(\theta_{t2} - \theta_s') - u_{1\,\mathrm{inf}}\,\sin\alpha\,(\sin\theta_{t2} + \sin\theta_s' - 2).$$

Note $\theta_s' > \theta_{t2}$ is impossible. We may also separate out asymmetric events by subtracting out the rate of double-peaked events as calculated above:

$$\Gamma_{\mathrm{asy}} = \Gamma_{\mathrm{dp+asy}} - \Gamma_{\mathrm{dp}}. \tag{A7}$$

Trajectories that take the MACHO no closer than $2d$ will yield light curves that look effectively like single star light curves. Therefore

$$\Gamma_{\mathrm{es}} = \Gamma_{\mathrm{binary}} - C2\pi d \qquad u_T < 2d,$$
$$\Gamma_{\mathrm{es}} = 0 \qquad u_T > 2d,$$

where C again is just a proportionality constant. The remaining events are categorized as borderline.

$$\Gamma_{\mathrm{bor}} = \Gamma_{\mathrm{binary}} - \Gamma_{\mathrm{es}} - \Gamma_{\mathrm{ob}} - \Gamma_{\mathrm{od}} - \Gamma_{\mathrm{mod}} - \Gamma_{\mathrm{dp}} - \Gamma_{\mathrm{asy}}. \tag{A8}$$

This completes the categorization scheme.

REFERENCES

Abt, H. A. 1983, ARA&A, 21, 343
Abt, H. A., Gomez, A. E., & Levy, S. G. 1990, ApJS, 74, 551 (AGL)
Abt, H. A., & Levy, S. G. 1976, ApJS, 30, 273
———. 1978, ApJS, 36, 241
———. 1985, ApJS, 59, 229 (AL)
Alcock, C. 1989, presentation at seminar at Center for Particle Astrophysics
Alcock, C., et al. 1991, in Robotic Telescopes in the 1990s, ed. A. V. Filippenko (ASP. Conf. Ser.), in press
Allen, C. W. 1973, Astrophysical Quantities (London: Athlone)
DeRujula, A., Jetzer, P., & Masso, E. 1990, CERN preprint CERN-TH-5812-90
Duquennoy, A., & Mayor, M. 1991, A&A, 248, 485
Ferlet, R., et al. 1990, Appendix to ESO Proposal, unpublished
Gould, A. 1992, ApJ, 388, 338
Griest, K. 1991, ApJ, 366, 412
Griffin, R. F. 1985, in Interacting Binaries, ed. P. P. Eggleton & J. E. Pringle (Dordrecht: Reidel), 1
Halbwachs, J. L. 1987, A&A, 183, 234
Jetzer, P. 1991, Zurich University preprint ZU-TH 15/91
Heintz, W. D. 1969, JRASC, 63, 275
Kuiper, G. P. 1935, PASP, 47, 121
Paczyński, B. 1986, ApJ, 304, 1
Paczyński, B., et al. 1991, private communication
Poveda, A., Allen, C., & Parrao, L. 1987, ApJ, 258, 589
Refsdal, S. 1964, MNRAS, 128, 295
Spiro, M. 1990, private communication
Tikhov, G. A. 1937, Dokl. Akad. Nauk. SSSR, 16, 199
Trimble, V. 1990, MNRAS, 242, 79
Wolff, S. C. 1978, ApJ, 222, 556
Zinnecker, H. 1984, Ap&SS, 99, 41

THE ASTROPHYSICAL JOURNAL, 407:440–441, 1993 April 10

ERRATUM

In the paper "Effect of Binary Sources on the Search for Massive Astrophysical Compact Halo Objects via Microlensing" by Kim Griest and Wayne Hu (ApJ, 397, 362 [1992]), an error occurs, which was pointed out by A. Milsztajn. Throughout, when transforming period distributions to star separation distributions M_T was used where M_T^{-1} should have been used. Correcting this error shifts the distributions by roughly a factor of 3 toward smaller binary star separations. Since the period distributions span a range of 10^{10}, this is not a large effect, but all the detailed numbers change.

Fortunately, the uncertainties introduced by the variations among the three different observational period distributions used are in most cases larger than the corrections noted here. The conclusions and the summary numbers given in the abstract, introduction, and §§ 1–4 are unchanged. (One exception is the percentage of events with color shifts larger than 0.1 mag which should read (in the Abstract) 3%–7% rather than 2%–5%). None of the figures change.

This erratum lists the changes which need to be made to §§ 5–8 and includes a new Table 4, where most of the numbers have changed. Qualitatively, the basic change is a shift of 5%–10% of the events from the "effectively single" category to the "offset bright" category. Smaller changes due to the shift in the bumps and wiggles in the observational period distributions, as well as smaller systematic changes can be gleaned from the new Table 4.

The formulae can be corrected by changing M_T to M_T^{-1} throughout. The Kepler formula should read $P^2 = a^3/M_T$, where the period P is in years, the semimajor axis a is in a.u., and the total mass M_T is in $M_\odot$. All factors of Newton's G should be ignored in these units. (Note, however, that the period bins in Table 3 are log P, with P in *days*.)

The following changes should be made: In § 5, all factors of $M_T^{1/2}$ should read $M_T^{-1/2}$. The second paragraph after equation (21) should read: "Thus we see the contributions from the various categories. The fraction of offset bright events ranges from 70%–81% at $m = 10^{-5}\ M_\odot$ to 49%–63% at $m = 10^{-1}\ M_\odot$. The fraction of separated offset dim events varies from between 7% and 22%, while the fraction of merged offset dim events varies from 0.4% to 2%. Double-peaked plus asymmetric events comprise from less than 1% to around 3% of the total, while essentially single events comprise between 1% and 37%, depending upon the MACHO mass and distribution used. Borderline events give between 1% and 7% of the total. Including the variation from all three distributions, the total percentage of probably distinguishable events ranges from 8% to 28%, with the more well-determined dark matter distribution, giving a 14%–19% range."

TABLE 4

EXPECTED FRACTION OF BINARY EVENTS BY CATEGORY

Mass ($M_\odot$)	ob	od	mod	dp+asy	es	bor	totd	$\langle\eta\rangle$
DM(F–G Stars) with A0 Primary								
10^{-5}	0.81	0.15	0.004	0.010	0.012	0.013	0.17–0.18	1.12
10^{-4}	0.78	0.14	0.007	0.015	0.035	0.022	0.16–0.19	1.11
10^{-3}	0.73	0.13	0.008	0.017	0.08	0.030	0.16–0.19	1.10
10^{-2}	0.68	0.12	0.010	0.021	0.13	0.040	0.15–0.19	1.09
10^{-1}	0.61	0.10	0.012	0.027	0.20	0.052	0.14–0.19	1.08
DM with A5 Primary								
10^{-3}	0.73	0.13	0.009	0.018	0.084	0.031	0.16–0.19	1.10
10^{-1}	0.60	0.10	0.013	0.027	0.21	0.055	0.14–0.19	1.08
DM with B5 Primary								
10^{-3}	0.74	0.13	0.008	0.016	0.066	0.031	0.16–0.19	1.11
10^{-1}	0.63	0.10	0.012	0.027	0.18	0.047	0.14–0.19	1.08
AGL(B Stars) with B5 Primary								
10^{-5}	0.81	0.099	0.010	0.024	0.012	0.042	0.13–0.18	1.08
10^{-4}	0.72	0.081	0.014	0.029	0.094	0.064	0.12–0.19	1.07
10^{-3}	0.62	0.078	0.007	0.016	0.21	0.073	0.10–0.17	1.06
10^{-2}	0.56	0.074	0.004	0.010	0.31	0.036	0.09–0.12	1.06
10^{-1}	0.53	0.070	0.003	0.009	0.37	0.023	0.08–0.10	1.05
Al(A stars) with A0 Primary								
10^{-5}	0.70	0.22	0.009	0.021	0.017	0.029	0.25–0.28	1.18
10^{-4}	0.66	0.20	0.013	0.023	0.066	0.030	0.24–0.27	1.16
10^{-3}	0.61	0.18	0.019	0.028	0.12	0.037	0.23–0.27	1.14
10^{-2}	0.55	0.16	0.018	0.030	0.19	0.052	0.21–0.26	1.12
10^{-1}	0.49	0.14	0.016	0.029	0.27	0.054	0.19–0.24	1.11

In § 6, the sentences in the second to last paragraph describing the color shift results should read: "For an A0 primary star and MACHO mass $m = 10^{-3}\ M_{\odot}$, we find $\sim 5.5\%$ of events will have a maximum $\Delta(B-V)$ of greater than 0.1 mag. For A5 and B5 stars, the fractions are 6.7% and 3.4%, respectively. For an A0 primary and $m = 10^{-5}\ M_{\odot}$, the fraction is 6.2%, while for an A0 with $m = 10^{-1}\ M_{\odot}$ it is 4.6%."

Finally, in § 8, the MACHO mass used in Figure 12 should be 4.3×10^{-3}, and the MACHO velocity needed to give such curves should be less than $v_{\perp} \sim 0.26 m^{-1/4} d^{-3/2}$, a factor of 3 larger than stated before: thus, $v_{\perp} = 2.1$ km s^{-1} in Figure 12. All conclusions drawn from the example are unchanged.